

4

Results

4.1 Isolation and screening of biosurfactant producing microorganisms

A total of 54 unique bacterial colonies and 2 fungal colonies were isolated by inoculating the petroleum-contaminated soil samples after performing serial dilution on Bushnell and Haas agar plates supplemented with 200 μL of diesel oil as the sole source of carbon. The morphological characteristics *i.e.*, color, shape, size, margin, surface, and elevation of all the isolates are depicted in **Table 4.1**. All the colonies with unique colony morphology were assigned unique IDs before final identification.

The best isolate with identity code 10J₃ was screened based on its ability to exert the maximum cell density ($9.23 \times 10^7 \pm 0.006$ cells/mL), dry cell biomass (0.816 ± 0.0006 mg/mL), and corresponding protein content (243.47 ± 0.83 $\mu\text{g/mL}$) in diesel oil-supplemented medium. It could also reduce the surface tension of hydrocarbon-supplemented medium (50.3 ± 0.08 mN/m) by 30 ± 0.006 % with respect to the control (72.1 mN/m) which confirmed its ability to produce biosurfactant. The results of the screening of all the isolates are presented in **Table 4.2**.

The isolate showed α -hemolysis on red blood cells which indicated its ability to produce bacterial biosurfactant (Fig. 4.1). Collapse of the drop of diesel oil-supplemented media on a hydrophobic surface within 45 sec indicates successful production of biosurfactant by the bacterial isolate (Fig. 4.2). The emulsification index of the cell-free extract was checked after 24 h of incubation with an equal volume of diesel and was determined as $35.71 \pm 0.09\%$ (Fig. 4.3).

4.2 Identification of the best isolate

4.2.1 Based on cell morphology

The best isolate 10J₃ was subjected to Gram staining and was observed under the 100X magnification of a light microscope using immersion oil. The isolate was found Gram-negative rod-shaped bacteria (Fig. 4.4).

4.2.2 Molecular identification of the best isolate

The best strain 10J₃ was identified as *Klebsiella sp.* based on 16S rDNA gene sequencing method out of 54 unique bacterial colonies isolated on diesel-supplemented BH agar. The strain name was given as *Klebsiella sp.* RGUDBI03 and GenBank accession no. ON945613.1 was successfully received from NCBI after the deposition of the sequence. The NCBI-BLAST hit shows maximum similarity (99.87%) of the strain with *Klebsiella pneumonia* with 100% query cover. The phylogenetic tree was constructed by aligning the top 10 hits from BLAST analysis using MEGAXTM software with 1000 bootstrap values and the maximum likelihood method. The isolate shows maximum similarity with *K. pneumonia* subsp. *quasipneumoniae* strain 01A030 and *K. pneumonia* strain DSM 30104 (Fig. 4.5).

4.3 Extraction and characterization of crude biosurfactant

The biosurfactant was extracted from the cell-free media of the best isolate by the cold acetone precipitation method. The appearance of a white powdery substance after vigorously stirring in the presence of chilled acetone indicated the precipitation of biosurfactant. Anthrone test of the crude biosurfactant showed the appearance of bluish green color indicating the presence of carbohydrate moieties in the

biosurfactant [97]. On the other hand, the appearance of a yellow color after performing the ninhydrin test confirmed the presence of amino acids specifically proline in the biosurfactant [97]. The FTIR spectral analysis of the crude biosurfactant further showed distinct peaks in the regions 3454.78, 3253.12, 2924.87, 1621.72, 1376.37, 1054.48, and 978.96 cm^{-1} attributed to the presence of O-H (bend), O-H (stretch), CH₂ (asymmetrical stretch), C=C (stretch), C-H (bend), C-H in-plane bends and C=C-H (bends) respectively (**Fig. 4.6**). Low and high-magnification images of SEM analysis show the surface morphology of the crude biosurfactant (**Fig. 4.7**).

4.4 Synthesis of Ag and ZnO NPs

The change in color of AgNO₃ solution from milky white to dark brown when reduced with biosurfactant confirmed the formation of Ag NPs. Similarly, the formation of a white precipitate when ZnCl₂ is reduced with biosurfactant confirmed the synthesis of ZnO NPs.

4.5 Characterization of the NPs

Scanning electron microscopic (SEM) analysis confirmed the successful synthesis of Ag NPs with uniform morphology (**Fig. 4.8a and b**), whereas EDX analysis confirmed the presence of metallic Ag NPs in the sample (**Fig. 4.8c**). The TEM analysis also shows well-dispersed Ag NPs (**Fig. 4.9a and b**) with a size range of 10- 40 nm (**Fig. 4.9c**). The HR-TEM image shows molecular fringes of 0.41 nm (**Fig. 4.9b**) in the single crystal Ag NPs and approximately 50% of the overall NPs exhibited the size range of 20-30 nm (**Fig. 4.9c**). The XRD results of Ag NPs show the presence of prominent peaks (2θ values) at 32.3° and 46.48° which corresponds to (111) and (200) planes of silver respectively, and thus confirming their crystalline nature (**Fig. 4.10**).

The FTIR spectra of Ag NPs showed distinct peaks in the regions 3444.82, 3380.72, 3131.67, 2922.3, 2448.81, 1641.96, 1384.40, 1261.26, 1118.97, 1074.64, 993.38, 956.61, 864.12, 825.45, 558.92, 538.30, and 517.64 cm^{-1} . The peaks have confirmed the presence of C=C-H, C-H (stretch), CH₂, C=C (stretch), C-H (bend), C-H (bend overtone), C=C-H (bends), and C-C (stretches) respectively in Ag NPs as

they were synthesized by reducing the metal salt with bacterial biosurfactant (**Fig. 4.11**). Differential thermal analysis (DTA) and thermogravimetric analysis (TGA) spectra of Ag NPs have recorded the weight loss of the NPs above 100 °C. There is almost no weight loss below 100 °C and above 500 °C (**Fig. 4.12**). DTA curves show a sharp peak at 100 °C, which corresponds with the results of TGA (**Fig. 4.12**).

Scanning electron microscopic (SEM) analysis confirmed the successful formation of ZnO NPs with uniform morphology (**Fig. 4.13a and b**), whereas EDX analysis confirms the presence of metallic ZnO NPs in the sample (**Fig. 4.13c**). The TEM analysis also shows well-dispersed ZnO NPs (**Fig. 4.14a and b**) with a size range of 2-10 nm (**Fig. 4.14c**). The HR-TEM image shows molecular fringes of 0.26 nm (**Fig. 4.14b**) in the single crystal ZnO NPs and approximately 50% of the overall NPs exhibited the size range of 2-4 nm (**Fig. 4.14c**). The XRD results of ZnO NPs show the presence of prominent peaks (2θ values) at 27.36°, 30.62° and 32.68° which corresponds to (200), (100), and (002) planes of zinc oxide respectively, and thus confirming their crystalline nature (**Fig. 4.15**) [258].

The FTIR spectra of ZnO NPs showed distinct peaks in the regions 3403.50, 1648.45, 1384.63, and 834.32 cm^{-1} . The peaks have confirmed the presence of C=C- H, C=C (stretch), C-H (bend), and C=C (stretch) respectively in ZnO NPs (**Fig. 4.16**) as they were synthesized by reducing the metal salt with bacterial biosurfactant [259]. Differential thermal analysis (DTA) and thermogravimetric analysis (TGA) spectra of ZnO NPs have shown similar observations as in Ag NPs which recorded the weight loss of the NPs above 100 °C (**Fig. 4.17**). There is almost no weight loss below 100 °C and above 500 °C (**Fig. 4.17**). DTA curves show a sharp peak at 100 °C, which corresponds with the results of TGA (**Fig. 4.17**).

4.6 Metal NPs mediated seed germination and plant growth assay

4.6.1 Seed water uptake assay

The chickpea and rice seeds were weighed after 3 h and 3 days of priming respectively to determine the seed water percentage of primed seeds. It was observed that the percentage of water uptake was higher in nano-primed seeds as compared to distilled water, biosurfactant, and AgNO_3 solution. The percentage of water uptake

also increases gradually for both the seeds with the increase in the concentration of the priming solution. The seed water uptake percentage of Ag NPs primed chickpea seeds at 10, 20, 30, and 40 mg/L dosage was obtained as 84.3 ± 0.09 , 86.25 ± 0.1 , 87.75 ± 0.06 , and $83.74 \pm 0.06\%$ respectively which was found significantly higher ($p < 0.05$) as compared to the values obtained for distilled water ($78.23 \pm 0.08\%$), biosurfactant ($72.2 \pm 0.17\%$) and different concentration of AgNO_3 (10 mg/L- $73.5 \pm 0.06\%$, 20 mg/L- $76.23 \pm 0.11\%$, 30 mg/L- $72.08 \pm 0.07\%$, and 40 mg/L- $76.6 \pm 0.09\%$). **Fig. 4.18** depicts the increase in the percentage of water uptake in Ag NPs primed chickpea seeds as the concentration of Ag NPs increases from 10 to 30 mg/L and decreases at 40 mg/mL of nano-primed dosage. The maximum water uptake achieved was $87.75 \pm 0.06\%$ at 30 mg/L concentrations of Ag NPs for chickpea seeds.

Similarly, the seed water uptake percentage of Ag NPs primed rice seeds at 10, 20, 30, and 40 mg/L of dosage was obtained as $74.83 \pm 0.5\%$, $82.8 \pm 0.55\%$, $85.6 \pm 0.68\%$, and $84 \pm 0.55\%$ respectively which was found significantly higher ($p < 0.05$) as compared to the respective control, *i.e.*, with distilled water ($44.68 \pm 0.05\%$), biosurfactant ($41.6 \pm 0.12\%$) and different concentration of AgNO_3 (10 mg/L- $55.43 \pm 0.57\%$, 20 mg/L- $57.13 \pm 0.44\%$, 30 mg/L- $43.81 \pm 0.5\%$, and 40 mg/L- $58.81 \pm 0.42\%$). The percentage of water uptake in rice seeds has significantly increased ($p < 0.05$) with a higher dosage of Ag NPs ranging from 10 to 30 mg/L and with no significant improvement in water uptake capacity at 40 mg/L of Ag NPs as represented in **Fig. 4.19**. The maximum water uptake achieved was $85.6 \pm 0.68\%$ at 30 mg/L concentrations of Ag NPs for rice seeds.

The percentage of water uptake was found higher in chickpea and rice seeds when primed with ZnO NPs as compared to distilled water, biosurfactant, and ZnCl_2 primed seeds. The water absorption capacity of both the seeds increased with the rise in the concentration of ZnO NPs priming solution. The seed water uptake percentage of primed chickpea seeds at 10, 20, 30, and 40 mg/L of ZnO NPs dosage was obtained as $78.37 \pm 0.07\%$, $85.77 \pm 0.06\%$, $89.06 \pm 0.06\%$, and $87.49 \pm 0.07\%$ respectively which was found significantly higher ($p < 0.05$) as compared to distilled water ($73.47 \pm 0.06\%$), biosurfactant ($72.2 \pm 0.17\%$) and different concentration of ZnCl_2 (10 mg/L- $74.21 \pm 0.06\%$, 20 mg/L- $80.57 \pm 0.06\%$, 30 mg/L- $79.17 \pm 0.05\%$, and 40 mg/L- $80.62 \pm 0.06\%$) (**Fig. 4.20**). The percentage of water uptake in ZnO NPs primed

chickpea seeds increases with the rise in the concentration from 10 to 30 mg/L and gradually reduces at 40 mg/L of nano-primed seeds which is shown in **Fig. 4.20**. The maximum water uptake achieved was $89.06 \pm 0.06\%$ at 30 mg/L of ZnO NPs primed chickpea seeds.

In the same way, the seed water uptake percentage of ZnO NPs primed rice seeds at 10, 20, 30, and 40 mg/L dosage was $76.8 \pm 0.5\%$, $82.8 \pm 0.5\%$, $92.54 \pm 0.5\%$, and $89.39 \pm 0.55\%$ respectively which was found significantly higher ($p < 0.05$) as compared to distilled water ($44.1 \pm 0.58\%$), biosurfactant ($41.6 \pm 0.12\%$) and different concentration of ZnCl₂ (10 mg/L- $72.8 \pm 0.5\%$, 20 mg/L- $77.83 \pm 0.45\%$, 30 mg/L- $79.11 \pm 0.47\%$, and 40 mg/L- $61.52 \pm 0.57\%$) treated seeds. As the concentration of ZnO NPs increases from 10 to 30 mg/L, the percentage of water uptake also increases but gradually declines at 40 mg/L of ZnO NPs priming solution (**Fig. 4.21**). The maximum water uptake was $92.54 \pm 0.5\%$ at 30 mg/L priming concentrations of ZnO NPs for rice seeds.

4.6.2 Germination percentage and length of the germinated seedlings

Both chickpea and rice seeds were incubated in dark conditions for the 3rd and 6th day respectively after priming with different concentrations of Ag NPs, AgNO₃, ZnO NPs, ZnCl₂, biosurfactant, and distilled water. On the 3rd and 6th day, each of the germinating chickpea and rice seeds respectively were measured to determine the total length of the germinated seedlings, and the germination percentage was determined. The germination percentage of chickpea and rice seeds was found higher in nano-primed seeds as compared to distilled water, biosurfactant, and AgNO₃ solution. The percentage of germination in Ag NPs primed chickpea seeds with 10, 20, 30, and 40 mg/L dosage was achieved as $94 \pm 0.8\%$, $96 \pm 0.7\%$, $98 \pm 0.89\%$, and $94 \pm 0.75\%$ respectively which was found significantly higher ($p < 0.05$) as compared to distilled water ($80 \pm 0.9\%$), biosurfactant ($80 \pm 0.7\%$) and different concentration of AgNO₃ (10 mg/L- $85 \pm 0.65\%$, 20 mg/L- $90 \pm 0.55\%$, 30 mg/L- $90 \pm 0.8\%$ and 40 mg/L- $85 \pm 0.8\%$) primed seeds (**Fig. 4.22**). The germination percentage in Ag NPs primed chickpea seeds significantly increases ($p < 0.05$) with an increase in the concentration from 10 to 30 mg/L and slightly reduces at 40 mg/L of Ag NPs primed seeds is shown in **Fig. 4.22**. The maximum germination percentage achieved was $98 \pm 0.89\%$ at 30

mg/L concentrations of Ag NPs for chickpea seeds. The growth of the seedlings with 10, 20, 30, and 40 mg/L of Ag NPs dosage was 35 ± 1 , 39.74 ± 0.9 , 45.45 ± 1.088 , and 43.95 ± 1.097 mm respectively which was found significantly higher ($p < 0.05$) as compared to distilled water (30.75 ± 1 mm), biosurfactant (29.7 ± 0.9 mm) and different concentration of AgNO_3 (10 mg/L- 30.26 ± 0.7 mm, 20 mg/L- 32.1 ± 0.8 mm, 30 mg/L- 39.5 ± 1.055 mm, and 40 mg/L- 37.5 ± 1.043 mm) primed seeds. The maximum average length achieved was 45.45 ± 1.09 mm at 30 mg/L concentration of Ag NPs on chickpeas and no significant increase in the growth of seedlings was observed when treated with 40 mg/L concentration (**Fig. 4.23**).

The percentage of germination in Ag NPs primed rice seeds was found $98 \pm 0.6\%$ at 10 mg/L priming dose and $94 \pm 0.5\%$ for 20 to 40 mg/L dosage, which was found significantly higher ($p < 0.05$) as compared to distilled water ($78 \pm 0.76\%$), biosurfactant ($78 \pm 0.6\%$) and different concentration of AgNO_3 (10 mg/L- $76 \pm 0.88\%$, 20 mg/L- $76 \pm 0.66\%$, 30 mg/L- $76 \pm 0.76\%$, and 40 mg/L- $66 \pm 0.55\%$) primed seeds. The highest percentage of germination was found $98 \pm 0.6\%$ at 10 mg/L concentration of Ag NPs in rice seeds, beyond which no significant enhancement in the germination percentage was observed (**Fig. 4.24**). The growth of the seedlings with 10, 20, 30, and 40 mg/L of Ag NPs dosage was found 17.75 ± 0.9 , 18.24 ± 0.85 , 20.63 ± 0.88 , and 20.68 ± 0.66 mm respectively, which was found significantly higher ($p < 0.05$) as compared to distilled water (13.13 ± 0.7 mm), biosurfactant (8.78 ± 0.9 mm) and different concentration of AgNO_3 (10 mg/L- 12.5 ± 0.5 , 20 mg/L- 10 ± 0.7 , 30 mg/L- 6.94 ± 0.65 , and 40 mg/L- 7 ± 0.55 mm) primed seeds. The maximum growth of the rice seedlings was found 20.63 ± 0.88 mm at 30 mg/L concentration of Ag NPs and no significant change in length was observed at 40 mg/L concentration (**Fig. 4.25**).

The germination percentage of ZnO NPs primed chickpea and rice seeds were found higher when compared with that of the control. The percentage of germination in chickpea seeds with 10, 20, 30, and 40 mg/L of ZnO NPs dosage was found $98 \pm 0.8\%$ which was significantly higher ($p < 0.05$) than that of the germination rates achieved by priming with distilled water ($80 \pm 0.9\%$), biosurfactant ($80 \pm 0.7\%$) and different concentration of ZnCl_2 (10 to 30 mg/L- $80 \pm 0.7\%$, and 40 mg/L- $85 \pm 0.8\%$). The percentage of germination in chickpea seeds remains constantly high at all dosages of ZnO NPs priming as represented in **Fig. 4.26**. The maximum germination

percentage achieved was $98\pm0.8\%$ and it remained the same for all the concentrations of ZnO NPs for chickpea seeds (**Fig. 4.26**). The growth of the seedlings with 10, 20, 30, and 40 mg/L of ZnO NPs dosage was achieved as 32.3 ± 0.9 , 35.25 ± 0.99 , 43.5 ± 1.03 , and 42.4 ± 1 mm respectively which was higher as compared to distilled water (30.75 ± 0.8 mm), biosurfactant (29.7 ± 0.9 mm) and different concentration of ZnCl₂ (10 mg/L- 28.85 ± 0.7 mm, 20 mg/L- 29 ± 0.88 mm, 30 mg/L- 38.35 ± 0.96 mm, and 40 mg/L- 36.95 ± 0.9 mm) primed seeds (**Fig. 4.27**). The maximum average length achieved was 43.5 ± 1.03 mm at 30 mg/L concentration of ZnO NPs on chickpea seedlings, beyond which no major changes in the growth of seedlings were observed at 40 mg/L concentration of ZnO NPs primed seeds (**Fig. 4.27**).

The percentage of germination in ZnO NPs primed rice seeds with 10, 20, 30, and 40 mg/L of dosage was found 50 ± 0.6 , 56 ± 0.55 , 60 ± 0.54 , and $76\pm0.45\%$ respectively which is significantly higher ($p < 0.05$) as compared to the germination percentage achieved with distilled water ($30\pm0.76\%$), biosurfactant ($30\pm0.6\%$) and different concentration of ZnCl₂ (10 mg/L- $40\pm0.88\%$, 20 mg/L- $42\pm0.66\%$, 30 mg/L- $34\pm0.76\%$, and 40 mg/L- $30\pm0.55\%$) primed seeds after the same duration of time. The percentage of germination was found to increase with the rise in concentration from 10 to 40 mg/L and maximum germination percentage was observed at 40 mg/L of ZnO NPs priming dose ($76\pm0.45\%$) (**Fig. 4.28**). The growth of the seedlings with 10, 20, 30, and 40 mg/L of Ag NPs dosage was found 22.22 ± 1.08 , 18.33 ± 1.07 , 13.57 ± 1.04 , and 18.33 ± 0.7 mm respectively which was found significantly higher ($p < 0.05$) as compared to distilled water (8.33 ± 0.81 mm), biosurfactant (8.78 ± 0.9 mm) and different concentration of ZnCl₂ (10 mg/L- 17.27 ± 0.6 , 20 mg/L- 14.7 ± 0.9 , 30 mg/L- 10 ± 1.73 , and 40 mg/L- 10.83 ± 1 mm) primed seeds. The maximum average growth of the seedlings was observed as 22.22 ± 1.08 mm at 10 mg/L concentration of ZnO NPs on rice seedlings and no significant increase in length was observed at 20 to 40 mg/L concentration of ZnO NPs on rice seeds (**Fig. 4.29**).

4.6.3 Alpha-amylase activity assay

The α -amylase activity of Ag NPs primed chickpea and rice seeds were estimated after 3rd and 6th day of incubation. The enzymatic activities of α -amylase in both seeds were found higher after priming with Ag NPs as compared to that of the control. The

α -amylase activity also increased gradually for both the seeds with the increase in the concentration of the priming solution. The α -amylase enzyme catalysis activity in chickpea seeds at 10, 20, 30, and 40 mg/L of Ag NPs dosage was determined as 0.26 ± 0.0024 , 0.3 ± 0.0024 , 0.33 ± 0.0024 , and 0.26 ± 0.0028 mg/g respectively which was found significantly higher ($p < 0.05$) as compared to distilled water (0.12 ± 0.0024 mg/g), biosurfactant (0.12 ± 0.0024 mg/g) and different concentration of AgNO_3 (10 mg/L- 0.13 ± 0.0048 mg/g, 20 mg/L- 0.2 ± 0.0037 mg/g, 30 mg/L- 0.18 ± 0.0024 mg/g, and 40 mg/L- 0.17 ± 0.0037 mg/g) primed seeds. **Fig. 4.30** represents the enhancement of α -amylase activity in Ag NPs primed chickpea seeds with the increase in the concentration of Ag NPs from 10 to 30 mg/L and slightly decreases at 40 mg/mL concentration. The maximum α -amylase activity (0.33 ± 0.0024 mg/g) was observed at a concentration of 30 mg/L of Ag NPs in chickpea seeds.

In the same way, the α -amylase activity of Ag NPs primed rice seeds at 10, 20, 30, and 40 mg/L concentration was found 1.02 ± 0.0072 , 1.29 ± 0.006 , 1.54 ± 0.006 , and 1.43 ± 0.0097 mg/g respectively which was found significantly higher ($p < 0.05$) as compared to the respective control, *i.e.*, distilled water (0.48 ± 0.0097 mg/g), biosurfactant (0.58 ± 0.006 mg/g) and different concentration of AgNO_3 (10 mg/L- 0.59 ± 0.006 mg/g, 20 mg/L- 0.87 ± 0.006 mg/g, 30 mg/L- 0.92 ± 0.005 mg/g, and 40 mg/L- 0.58 ± 0.006 mg/g) primed seeds (**Fig. 4.31**). The enzyme activity in rice seeds significantly increased with higher dosages of Ag NPs ranging from 10 to 30 mg/L and slightly decreased at 40 mg/L concentration (**Fig. 4.31**). The highest α -amylase activity (1.54 ± 0.006 mg/g) was found at 30 mg/L of Ag NPs.

The α -amylase activity in ZnO NPs primed chickpea seeds at 10, 20, 30, and 40 mg/L of dosage was found 0.25 ± 0.0048 , 0.32 ± 0.0048 , 0.37 ± 0.0024 , and 0.3 ± 0.0037 mg/g respectively which was found significantly higher ($p < 0.05$) as compared to distilled water (0.11 ± 0.0028 mg/g), biosurfactant (0.12 ± 0.0024 mg/g) and different concentration of ZnCl_2 (10 mg/L- 0.12 ± 0.0048 mg/g, 20 mg/L- 0.13 ± 0.0028 mg/g, 30 mg/L- 0.18 ± 0.0024 mg/g, and 40 mg/L- 0.13 ± 0.005 mg/g) primed seeds (**Fig. 4.32**). As the concentration of ZnO NPs dosage increases from 10 to 30 mg/L, the α -amylase activity also increases (**Fig. 4.32**). However, no further significant enhancement in enzyme activity was observed at 40 mg/mL dose of ZnO NPs on chickpea (**Fig. 4.32**). The maximum α -amylase activity was determined as

0.37±0.0024 mg/g at 30 mg/L priming concentrations of ZnO NPs for chickpea seeds (**Fig. 4.32**).

Similarly, the α -amylase activity of ZnO NPs primed rice seeds at 10, 20, 30, and 40 mg/L concentration was found 1.65±0.0097, 2.17±0.009, 2.49±0.0064, and 2.39±0.0084 mg/g respectively which was found significantly higher ($p < 0.05$) as a comparison to distilled water (0.97±0.00843 mg/g), biosurfactant (0.58±0.006 mg/g) and different concentration of ZnCl₂ (10 mg/L- 1.2±0.0097 mg/g, 20 mg/L- 1.9±0.0097 mg/g, 30mg/L- 2.05±0.0073 mg/g, and 40 mg/L- 1.44±0.0055 mg/g) primed seeds (**Fig. 4.33**). The increase in the concentration of ZnO NPs from 10 to 30 mg/L enhances the α -amylase activity but no significant improvement in the enzymatic activity was observed at 40 mg/L of ZnO NPs priming solution (**Fig. 4.33**). The maximum α -amylase activity was recorded as 2.49±0.0063 mg/g at 30 mg/L priming concentrations of ZnO NPs in rice seeds.

4.6.4 Total soluble sugar content

The soluble sugar content also increases gradually for both seeds with the increase in the concentration of the priming solution. The amount of sugar content in chickpea seeds at 10, 20, 30, and 40 mg/L of Ag NPs dosage was found 10.83±0.12, 12.28±0.07, 12.5±0.06, and 10.6±0.05 μ g/mL respectively which is significantly higher ($p < 0.05$) as compared to distilled water (7.6±0.08 μ g/mL), biosurfactant (7.1±0.02 μ g/mL) and different concentration of AgNO₃ (10 mg/L- 8.8±0.08 μ g/mL, 20 mg/L- 11.11±0.05 μ g/mL, 30 mg/L- 10.6±0.08 μ g/mL, and 40 mg/L- 8.31±0.06 μ g/mL) primed seeds. **Fig. 4.34** shows the enhancement of soluble sugar content in Ag NPs primed chickpea seeds with the increase in concentration of Ag NPs from 10 to 30 mg/L, beyond which no increase in the sugar content was observed. The maximum sugar content observed was 12.5±0.058 μ g/mL at a concentration of 30 mg/L Ag NPs in chickpea seeds (**Fig. 4.34**).

Similarly, the amount of total soluble sugar content in Ag NPs primed rice seeds at 10, 20, 30, and 40 mg/L concentration was found 7.65±0.05, 8.23±0.06, 9.6±0.06, and 9.5±0.06 μ g/mL respectively which is significantly high as compared to the respective control, *i.e.*, distilled water (6.17±0.06 μ g/mL), biosurfactant

(4.86 ± 0.06 $\mu\text{g/mL}$) and different concentration of AgNO_3 (10 mg/L- 6.7 ± 0.07 $\mu\text{g/mL}$, 20 mg/L- 5.7 ± 0.06 $\mu\text{g/mL}$, 30 mg/L- 8.67 ± 0.08 $\mu\text{g/mL}$, and 40 mg/L- 7.68 ± 0.07 $\mu\text{g/mL}$) primed seeds (**Fig. 4.35**). The soluble sugar content in rice seeds has significantly increased ($p < 0.05$) with higher dosages of Ag NPs ranging from 10 to 30 mg/L and decreased in 40 mg/L concentration as shown in **Fig. 4.35**. The highest amount of total soluble sugar for rice seeds was observed to be 9.6 ± 0.06 $\mu\text{g/mL}$ when primed with 30 mg/mL of Ag NPs.

The concentration of soluble sugar of ZnO NPs primed chickpea seeds at 10, 20, 30, and 40 mg/L dosage was found 10.85 ± 0.05 , 11.22 ± 0.07 , 12.23 ± 0.087 , and 10.6 ± 0.18 $\mu\text{g/mL}$ respectively which was found significantly high ($p < 0.05$) as compared to distilled water (6.73 ± 0.06 $\mu\text{g/mL}$), biosurfactant (4.86 ± 0.06 $\mu\text{g/mL}$) and different concentration of ZnCl_2 (10 mg/L- 8.9 ± 0.057 $\mu\text{g/mL}$, 20 mg/L- 5.76 ± 0.058 , 30 mg/L- 10.6 ± 0.06 $\mu\text{g/mL}$, and 40 mg/L- 8.64 ± 0.051 $\mu\text{g/mL}$) primed seeds. As the concentration of ZnO NPs dosage increases from 10 to 30 mg/L, the amount of sugar also increases but again decreases at 40 mg/mL concentration of the primed solution in chickpea seeds (**Fig. 4.36**). The highest sugar content was determined as 12.23 ± 0.08 $\mu\text{g/mL}$ at 30 mg/L priming concentration of ZnO NPs in chickpea seeds.

Similarly, the sugar content of ZnO NPs primed rice seeds at 10, 20, 30, and 40 mg/L dosage was found 9.52 ± 0.07 , 9.94 ± 0.08 , 11.9 ± 0.07 , and 9.4 ± 0.07 $\mu\text{g/mL}$ respectively and was found significantly high ($p < 0.05$) as compared to distilled water (6.73 ± 0.06 $\mu\text{g/mL}$), biosurfactant (4.86 ± 0.058 $\mu\text{g/mL}$) and different concentration of ZnCl_2 (10 mg/L- 1.45 ± 0.06 $\mu\text{g/mL}$, 20 mg/L- 3.66 ± 0.09 $\mu\text{g/mL}$, 30 mg/L- 4.84 ± 0.06 $\mu\text{g/mL}$, and 40 mg/L- 5.69 ± 0.06 $\mu\text{g/mL}$) primed seeds. The increase in the concentration of ZnO NPs from 10 to 30 mg/L enhanced the amount of total soluble sugar content in seeds but decreased at 40 mg/L concentration of ZnO NPs priming solution (**Fig. 4.37**). The maximum soluble sugar content was found 11.9 ± 0.07 $\mu\text{g/mL}$ at 30 mg/L of priming concentrations for rice seeds.

The overall growth of chickpea and rice seedlings after treating with the priming solution at different time interval is depicted in **Fig. 4.38a-d**.

4.7 Cytotoxicity effect of the synthesized NPs

The possible cytotoxic effect of Ag NPs and ZnO NPs was tested on red blood cells and found non-hemolytic (**Fig. 4.39** and **Fig. 4.40**). The hemolytic activity in the presence of 10, 20, 30, and 40 mg/L doses of Ag NPs on red blood cells was found 0.042 ± 0.001 , 0.99 ± 0.007 , 0.94 ± 0.003 , $0.59\pm 0.001\%$ respectively. Similarly, 10, 20, 30, and 40 mg/L doses of ZnO NPs showed 0.85 ± 0.005 , 0.8 ± 0.001 , 1.17 ± 0.002 , and $1.13\pm 0.002\%$ hemolytic activity respectively.

4.8 Environmental toxicity assessment by taking earthworms as indicator

The treated earthworms in both the control and test groups were found to have no death, no color, and behavioral changes which showed no ecotoxic nature of the Ag NPs and ZnO NPs (**Table 4.3** and **4.4**). The histological staining result of both the control (**Fig. 4.41a**) and test (**Fig. 4.41b** and **Fig. 4.42b**) shows the presence of healthy villi (V) in the gut tissues of the earthworms. In addition to this, the treated earthworms also showed normal reproduction with offspring even after treatment with the NPs.

4.9 Antimicrobial activity of Ag NPs and ZnO NPs against plant pathogens

The antimicrobial potential of Ag NPs and ZnO NPs was determined initially by well diffusion against *Ralstonia solanacearum* F1C1 and *Fusarium oxysporum* f. sp. *pisi* (van Hall) Snyder & Hansen strain 4814. The Ag NPs showed antimicrobial activity against *Ralstonia solanacearum* F1C1 with a zone of inhibition of 16 ± 1 mm, whereas, 1 mM AgNO₃ and 5 mg/mL concentration of biosurfactant showed no zone of inhibition against the same strain (**Fig. 4.43**). Similarly, Ag NPs exhibited antimicrobial activity against *Fusarium oxysporum* f. sp. *pisi* (van Hall) Snyder & Hansen strain 4814 with a zone of inhibition of 22 ± 1 mm (**Fig. 4.44**). However, 1 mM AgNO₃ and 5 mg/mL concentration of biosurfactant showed no antimicrobial effect against this strain.

The Ag NPs exhibited an antimicrobial effect against *Ralstonia solanacearum* F1C1 with MIC value of 0.07 mg/mL and MBC value of 0.1 mg/mL. The MIC and MBC value against *Fusarium oxysporum* f. sp. *pisi* (van Hall) Synder & Hansen strain 4814 was evaluated as 0.04 and 0.09 mg/mL respectively (**Table 4.5**).

In contrast, ZnO NPs showed no antimicrobial effect against both *Ralstonia solanacearum* F1C1, and *Fusarium oxysporum* f. sp. *pisi* (van Hall) Synder & Hansen strain 4814 (**Fig. 4.32**).

Table 4.1 Colony characterization of the bacterial isolates

Sample ID	Location	Latitude	Longitude	Colony ID	No. of colonies	Shape	Size	Margin	Surface	Elevation	Colour
A	Boragaon	26.1167° N	91.6828°E	A ₁	2	Round	Medium	Entire	Rough	Flat	Transparent
				A ₂	2	Irregular	Medium	Undulate	Smooth	Raised	White
				A ₃	7	Irregular	Medium	Undulate	Smooth	Flat	White
				A ₄	2	Irregular	Large	Lobate	Rough	Flat	Transparent
				A ₅	19	Irregular	Small	Undulate	Rough	Raised	White
				A ₆	14	Round	Small	Entire	Smooth	Raised	White
				A ₇	3	Round	Small	Entire	Rough	Flat	Transparent
				A ₈	-	Round	Very Small	Entire	Rough	Flat	White
B				B ₁	23	Irregular	Small	Entire	Smooth	Flat	White
C	Lakhra	26.116°N	91.7496°E	C ₁	16	Round	Small	Entire	Smooth	Raised	White
D				D ₁	1	Irregular	Large	Undulate	Smooth	Flat	White
				D ₂	-	Round	Very Small	Entire	Smooth	Raised	Transparent
				D ₃	3	Round	Small	Entire	Smooth	Raised	White
E	Jyutikuchi	26.1285°N	91.7320°E	E ₁	3	Round	Small	Entire	Smooth	Raised	White
				E ₂	1	Round	Small	Entire	Rough	Raised	Transparent
				E ₃	1	Round	Small	Entire	Smooth	Raised	Creamish White
F				F ₁	32	Irregular	Medium	Entire	Smooth	Flat	White
				F ₂	1	Irregular	Medium	Undulate	Rough	Flat	Transparent
G	Beltola	26.1286°N	91.8013°E	G ₁	-	Irregular	Medium	Entire	Smooth	Flat	White
H				H ₁	12	Irregular	Medium	Entire	Smooth	Flat	White
					H ₂	29	Round	Small	Entire	Smooth	Raised

I	Lalganesh	26.1417°N	91.7454°E	I ₁	3	Round	Medium	Entire	Smooth	Raised	Orange	
				I ₂	6	Round	Small	Entire	Rough	Flat	Orange	
				I ₃	2	Irregular	Medium	Undulate	Smooth	Raised	White	
				I ₄	8	Round	Medium	Entire	Rough	Flat	White	
				I ₅	25	Round	Small	Entire	Smooth	Raised	White	
J				J ₁	3	Round	Small	Entire	Smooth	Raised	Reddish Pink	
				J ₂	19	Round	Small	Entire	Smooth	Raised	Yellow	
				J ₃	18	Round	Medium	Entire	Rough	Flat	White	
				J ₄	56	Round	Small	Entire	Smooth	Raised	Creamish white	
K	Fatashil	26.1663°N	91.7367°E	K ₁	1	Irregular	Medium	Entire	Rough	Flat	Transparent	
				K ₂	3	Irregular	Medium	Entire	Rough	Flat	White	
L				L ₁	3	Round	Medium	Entire	Rough	Raised	White	
				L ₂	Fungus	-	-	-	-	-	-	Green
				L ₃	20	Round	Small	Entire	Smooth	Raised	Yellow	
				L ₄	30	Round	Medium	Entire	Rough	Raised	White	
M	Ambari	26.1837°N	91.7533°E	M ₁	13	Round	Small	Entire	Smooth	Raised	Yellow	
				M ₂	3	Round	Medium	Entire	Rough	Flat	White	
				M ₃	25	Round	Medium	Entire	Smooth	Raised	White	
N				N ₁	7	Irregular	Medium	Entire	Rough	Flat	Transparent	
				N ₂	29	Round	Small	Entire	Smooth	Raised	White	
O	Ahomgaon	26.1059°N	91.7321°E	O ₁	3	Irregular	Large	Undulate	Rough	Flat	White	
				O ₂	Fungus	-	-	-	-	-	-	White
				O ₃	Fungus	-	-	-	-	-	-	White
				O ₄	12	Round	Medium	Entire	Smooth	Raised	White	
P				P ₁	-	Irregular	Medium	Undulate	Smooth	Raised	Yellow	
				P ₂	-	Irregular	Medium	Undulate	Smooth	Raised	White	

Q	Rihabari	26.1734°N	91.7472°E	Q ₁	4	Irregular	Small	Entire	Rough	Flat	Transparent
				Q ₂	1	Irregular	Medium	Entire	Smooth	Flat	White
R				R ₁	7	Irregular	Small	Entire	Smooth	Flat	Yellowish white
				R ₂	6	Round	Small	Entire	Smooth	Raised	White
				R ₃	3	Round	Small	Entire	Smooth	Raised	White
S	Aathgaon	26.1732°N	91.7394°E	S ₁	5	Round	Small	Entire	Rough	Raised	White
				S ₂	4	Round	Small	Entire	Rough	Raised	Pink
				S ₃	1	Irregular	Medium	Entire	Rough	Raised	Transparent
T				T ₁	1	Irregular	Large	Entire	Rough	Flat	Transparent
				T ₂	1	Round	Small	Entire	Rough	Raised	Transparent

Table 4.2 Screening of the best isolate

Sample ID	CFU (x10⁷)	Cell dry biomass (mg/mL)	Protein content (µg/mL)	Surface tension (mN/m)	Surface tension reduction (%)
1A ₁	3.7±0.1	0.049±0.002	75.87 ± 0.023	65.6 ± 0.01	9.01 ± 0.01
1A ₂	4.37±0.01	0.096±0.001	78.53 ± 1.89	68 ± 1	5.69 ± 0.02
1A ₃	1.95±0.02	0.016±0.001	28.67 ± 0.23	70 ± 3	2.91 ± 0.03
1A ₄	3.51±0.04	0.015±0.001	86.67 ± 5.67	65 ± 1	9.85 ± 0.02
1A ₅	1.19±0.03	0.019±0.001	27.33 ± 0.23	70.2 ± 0.53	2.63 ± 0.03
1A ₆	3.35±0.04	0.032±0.001	79.07 ± 0.61	68.2 ± 0.2	5.4 ± 0.2
1A ₇	1.37±0.03	0.015±0.006	48.80 ± 0.40	62 ± 2	14 ± 0.6
1A ₈	8.7±0.01	0.031±0.009	168.27 ± 3.00	50.6 ± 0.035	29.82 ± 0.07
2B ₁	1.6±0.06	0.005±0.001	38.4 ± 1.74	69.2 ± 0.2	4.02 ± 0.07
3C ₁	1.58±0.09	0.005±0.001	23.47 ± 0.61	70.4 ± 0.2	2.36 ± 0.04
4D ₁	1.15±0.05	0.006±0.001	29.33 ± 0.61	70.1 ± 0.5	2.77 ± 0.03
4D ₂	3.21±0.07	0.019±0.005	55.6 ± 1.83	64 ± 1	11.23 ± 0.06
4D ₃	3.57±0.05	0.02±0.007	85.6 ± 0.28	65.2 ± 0.2	9.57 ± 0.05
5E ₁	1.51±0.04	0.017±0.007	27.07 ± 0.23	70.33 ± 0.2	2.5 ± 0.04
5E ₂	2.47±0.07	0.705±0.004	60.67 ± 1.67	65.4 ± 0.2	9.29 ± 0.06
5E ₃	0.95±0.05	0.726±0.004	37.73 ± 0.23	69.7 ± 0.02	3.32 ± 0.04
6F ₁	1.8±0.06	0.016±0.004	30.8 ± 0.4	63.5 ± 0.4	11.92 ± 0.04
6F ₂	4.01±0.04	0.788±0.008	57.2 ± 2.23	66.43 ± 0.06	7.86 ± 0.02
7G ₁	3.54±0.05	0.011±0.003	70.8 ± 1.2	68 ± 1	5.69 ± 0.04
8H ₁	1.94±0.04	0.019±0.004	46.67 ± 0.23	63.3 ± 0.6	12.2 ± 0.4
8H ₂	5.06±0.03	0.018±0.005	105.73 ± 1.62	58.6 ± 0.3	18.72 ± 0.02
9I ₁	1.77±0.2	0.014±0.005	35.6 ± 0.8	70.6 ± 0.03	2.08 ± 0.02
9I ₂	2.6±0.07	0.014±0.005	43.73 ± 0.23	63.3 ± 0.6	12.2 ± 0.05
9I ₃	2.41±0.08	0.031±0.006	54.53 ± 0.46	68.5 ± 0.05	4.99 ± 0.07
9I ₄	2.81±0.08	0.019±0.005	49.87 ± 0.61	69.2 ± 0.05	4.02 ± 0.01
9I ₅	2.79±0.02	0.004±0.001	50 ± 0.8	68 ± 1	5.69 ± 0.07
10J ₁	5.28±0.02	0.005±0.001	49.33 ± 0.46	68.7 ± 0.04	4.71 ± 0.07
10J ₂	3.96±0.02	0.03±0.01	86.8 ± 0.82	62.87 ± 0.02	12.8 ± 0.09
10J ₃	9.23±0.01	0.816±0.001	243.47 ± 0.83	50.3 ± 0.08	30.23 ± 0.01
10J ₄	1.56±0.04	0.028±0.008	34.53 ± 0.23	69.4 ± 0.05	3.74 ± 0.04

11K ₁	1.62±0.02	0.007±0.001	35.6 ± 0.52	67.4 ± 0.06	6.51 ± 0.03
11K ₂	2.66±0.03	0.002±0.001	62.93 ± 0.61	66.1 ± 0.06	8.32 ± 0.02
12L ₁	5.58±0.03	0.017± 0.005	159.07 ± 1.29	56.77 ± 0.01	21.26 ± 0.02
12L ₃	2.59±0.04	0.019±0.006	70.13 ± 0.46	68.3 ± 0.04	5.27 ± 0.02
12L ₄	3.11±0.04	0.005±0.001	86.53 ± 1.01	64.6 ± 0.2	10.4 ± 0.05
13M ₁	2.19±0.02	0.006±0.001	52.27 ± 0.23	69.81 ± 0.03	3.18 ± 0.01
13M ₂	1.75±0.04	0.007±0.001	30 ± 1.2	69.72 ± 0.05	3.3 ± 0.05
13M ₃	2.36±0.02	0.008±0.001	54.53 ± 0.46	64 ± 1	11.23 ± 0.05
14N ₁	5.16±0.04	0.038± 0.008	139.47 ± 5.06	55.12 ± 0.055	23.55 ± 0.06
14N ₂	7.19±0.07	0.026±0.004	150.4 ± 7.47	55.9 ± 0.06	22.47 ± 0.02
15O ₁	5.28±0.06	0.029±0.004	77.47 ± 1.02	66.4 ± 0.02	7.9 ± 0.05
15O ₄	2.09±0.05	0.044±0.004	40.8 ± 0.69	63 ± 1	12.62 ± 0.07
16P ₁	2.43±0.05	0.018±0.002	48.93 ± 0.83	64.11 ± 0.07	11.08 ± 0.01
16P ₂	2.06±0.04	0.024 ±0.004	50.4 ± 1.44	60.8 ± 0.0802	15.67 ± 0.04
17Q ₁	1.45±0.05	0.02±0.004	41.87 ± 0.23	65 ± 1	9.85 ± 0.04
17Q ₂	1.46±0.03	0.009±0.001	42.53 ± 0.23	67.65 ± 0.03	6.17 ± 0.02
18R ₁	2.21±0.05	0.01±0.005	43.6 ± 0.4	66.55 ± 3.46	7.56 ± 0.03
18R ₂	2.73±0.05	0.017±0.003	61.73 ± 1.04	61.09 ± 0.05	15.27 ± 0.07
18R ₃	1.88±0.02	0.024±0.004	48 ± 0.4	69.74 ± 0.54	3.27 ± 0.04
19S ₁	2.23±0.03	0.044±0.005	56.27 ± 0.23	36.9 ± 0.22	2.71 ± 0.04
19S ₂	1.74±0.04	0.012±0.005	31.87 ± 0.61	70 ± 1	2.91 ± 0.06
19S ₃	2.53±0.06	0.019±0.005	46.13 ± 0.23	63.77 ± 1.74	11.55 ± 0.03
20T ₁	2.79±0.06	0.002±0.001	59.87 ± 0.92	60.23 ± 0.03	16.46 ± 0.03
20T ₂	2.57±0.04	0.022±0.002	60.4 ± 0.4	60.44 ± 0.02	16.17 ± 0.04

Table 4.3 Result of soil toxicity assessment on earthworms (*Eudrilus eugeniae*) at different concentrations of Ag NPs

Sl. no	Parameter analysed	Control (DW)	Ag NPs (10 mg/L)	Ag NPs (20 mg/L)	Ag NPs (30 mg/L)	Ag NPs (40 mg/L)
1	Colour change	No	No	No	No	No
2	Behavioural change	No	No	No	No	No
3	Death	No	No	No	No	No
4	Reproduction	Yes	Yes	Yes	Yes	Yes

Table 4.4 Result of soil toxicity assessment on earthworms (*Eudrilus eugeniae*) at different concentrations of ZnO NPs

Sl. no	Parameter analysed	Control (DW)	ZnO NPs (10 mg/L)	ZnO NPs (20 mg/L)	ZnO NPs (30 mg/L)	ZnO NPs (40 mg/L)
1	Colour change	No	No	No	No	No
2	Behavioural Change	No	No	No	No	No
3	Death	No	No	No	No	No
4	Reproduction	Yes	Yes	Yes	Yes	Yes

Table 4.5 Antimicrobial activity of metal NPs against some plant pathogens

Sl. No.	Name of NPs used	Plant pathogen	Zone of Inhibition (mm)	MIC (mg/mL)	MBC (mg/mL)
1	Ag NPs	<i>Ralstonia solanacearum</i>	16 ± 1	0.07	0.1
2	AgNO ₃	<i>Ralstonia solanacearum</i>	Resistant	-	-
3	ZnO NPs	<i>Ralstonia solanacearum</i>	Resistant	-	-
4	ZnCl ₂	<i>Ralstonia solanacearum</i>	Resistant	-	-
5	Ag NPs	<i>Fusarium oxysporum</i>	22 ± 1	0.04	0.09
6	AgNO ₃	<i>Fusarium oxysporum</i>	Resistant	-	-
7	ZnO NPs	<i>Fusarium oxysporum</i>	Resistant	-	-
8	ZnCl ₂	<i>Fusarium oxysporum</i>	Resistant	-	-

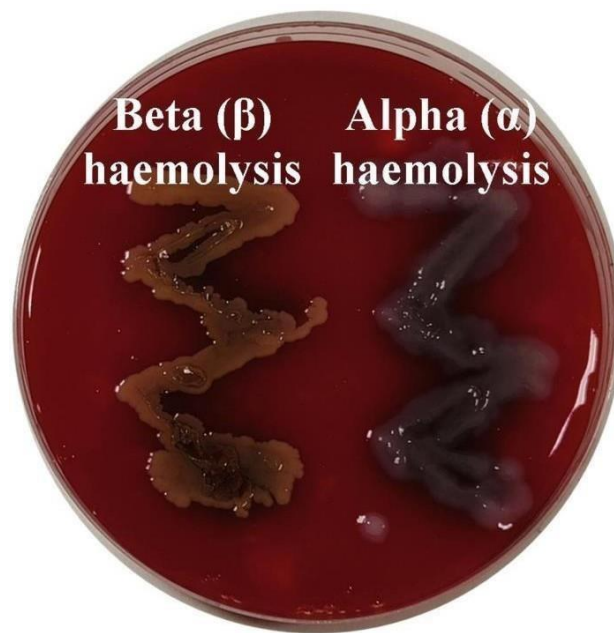


Fig. 4.1 Beta (β) and alpha (α) haemolysis shown by *Staphylococcus aureus* (control) and isolate 10J3 respectively on blood agar

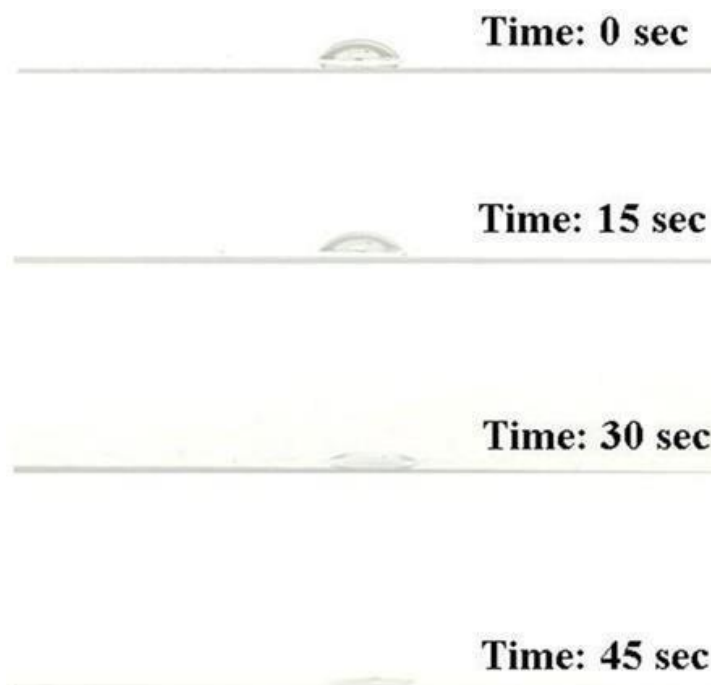


Fig. 4.2 Drop collapse test result of diesel supplemented BH broth after treating with the isolate 10J₃ at different time interval

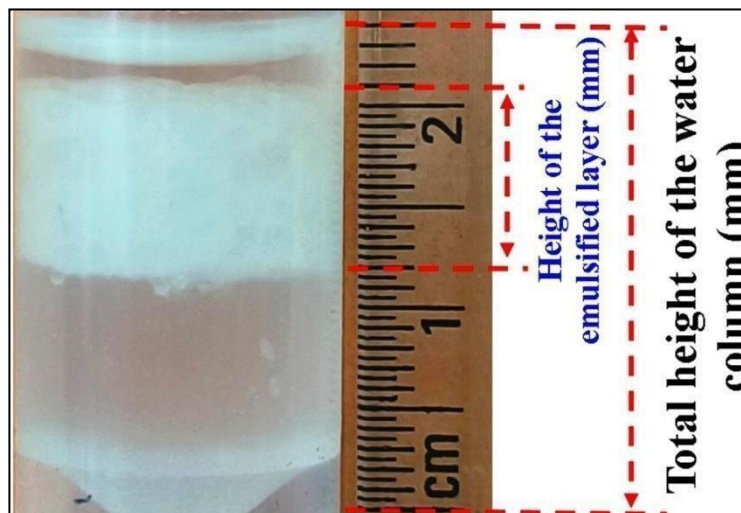


Fig. 4.3 Result of emulsification index (E_{24}) of the bacterial cell free extract with equal volume of diesel oil showing the height of the emulsified layer after 24 h of incubation

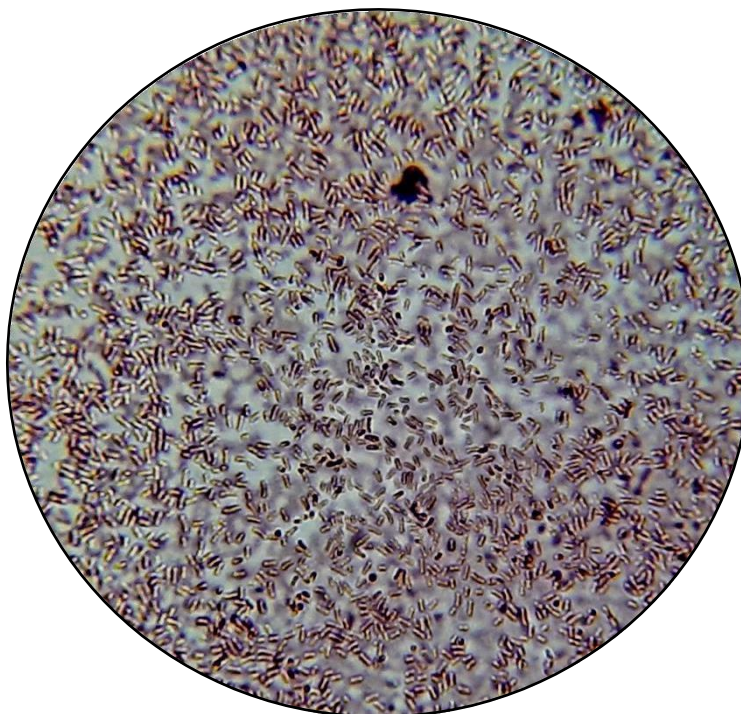


Fig. 4.4 Grams staining result of the isolate 10J₃ showing gram negative rods



Fig. 4.5 Phylogenetic position of *Klebsiella sp.* strain RGUDBI03 (GenBank accession: ON945613.1) (isolate 10J₃) with 10 most closely related strains and taking *Bacillus cereus* strain DRDU1 as outgroup. The respective Genbank accession numbers are indicated at the beginning of each species. The tree was constructed based on maximum likelihood method with 1000 bootstrap value. Abbreviation of culture collections are DSM: Deutsche Sammlung von Mikroorganismen und Zellkulturen, Germany and NBRC: NITE Biological Resource Center, Japan

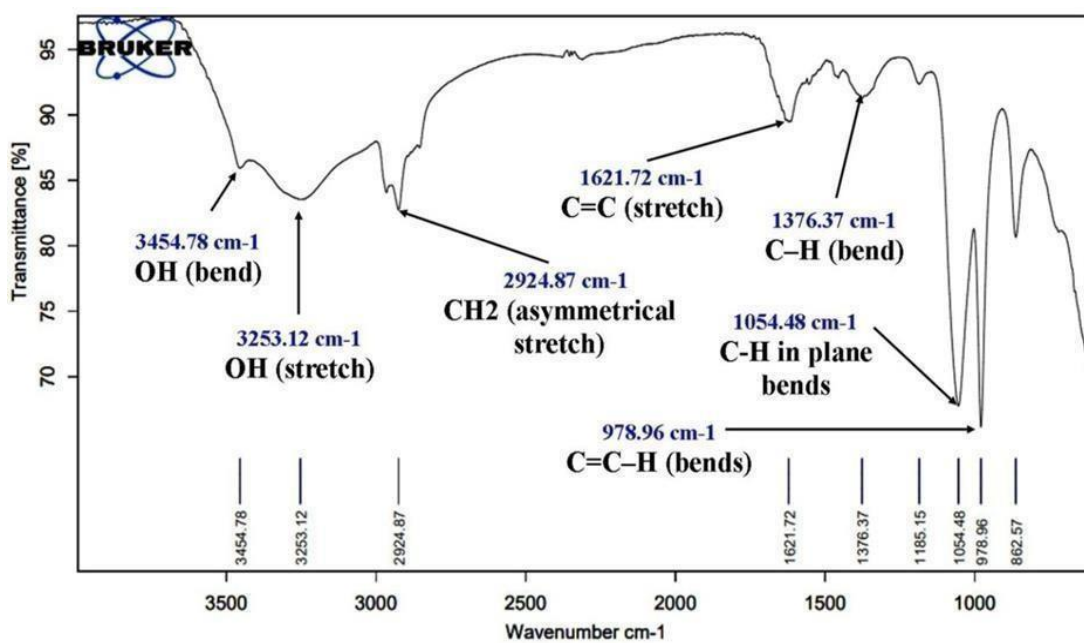


Fig. 4.6 FTIR spectra of the crude biosurfactant produced by the isolate 10J₃ showing the presence of various functional groups

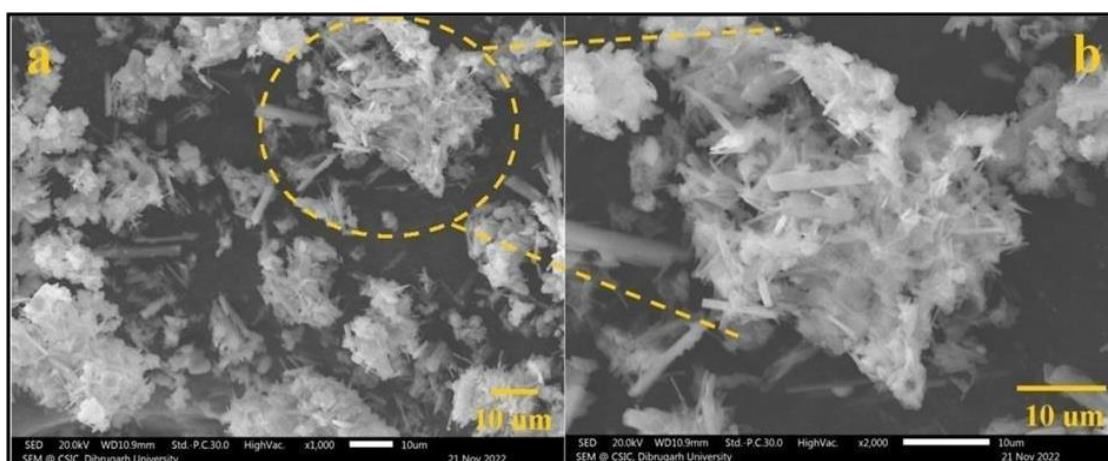


Fig. 4.7 SEM images of biosurfactant produced by the isolate 10J₃ under (a) low and (b) high magnification

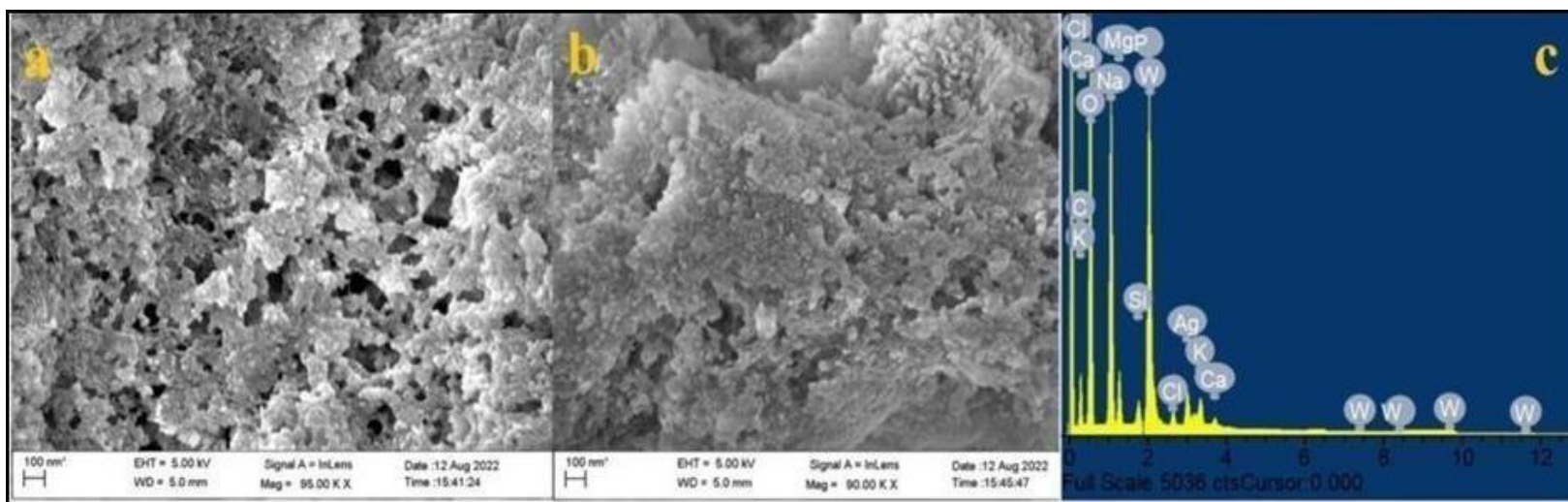


Fig. 4.8 SEM images of (a-b) Ag NPs and (c) EDX spectra

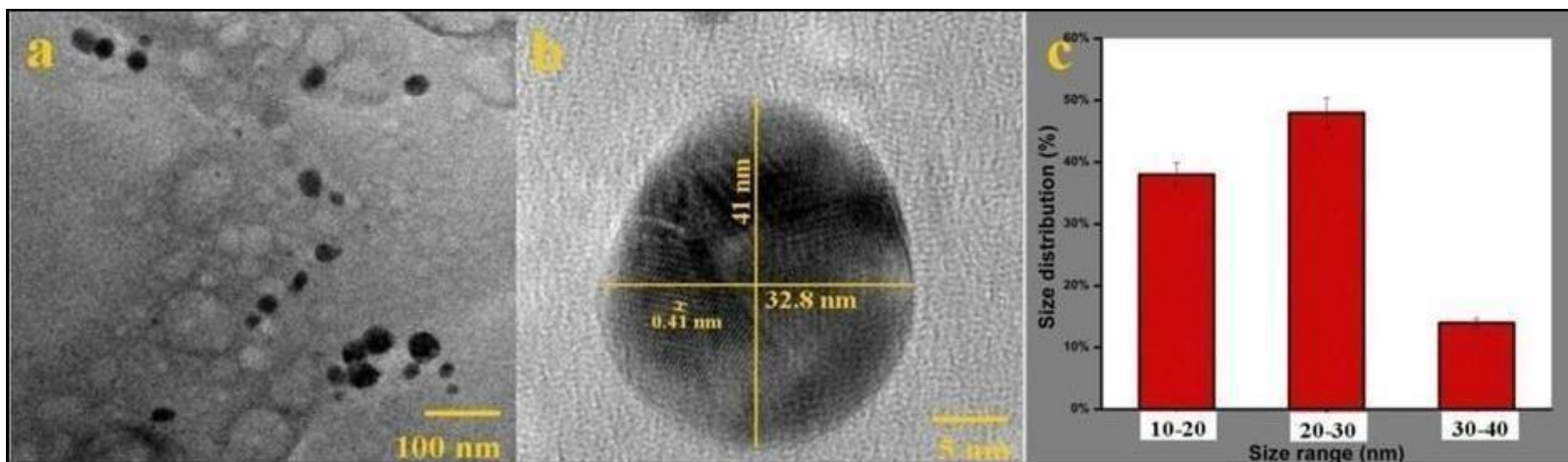


Fig. 4.9 TEM images of Ag NPs at (a) low and (b) high magnification and (c) size distribution graph of the NPs

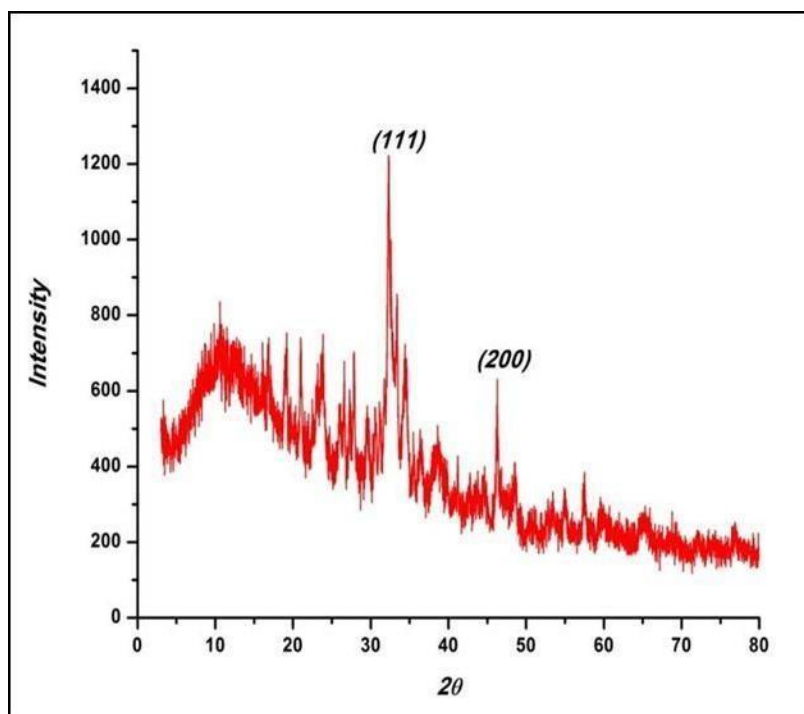


Fig. 4.10 The peaks obtained from XRD spectra showing the fcc lattice points in the Ag NPs

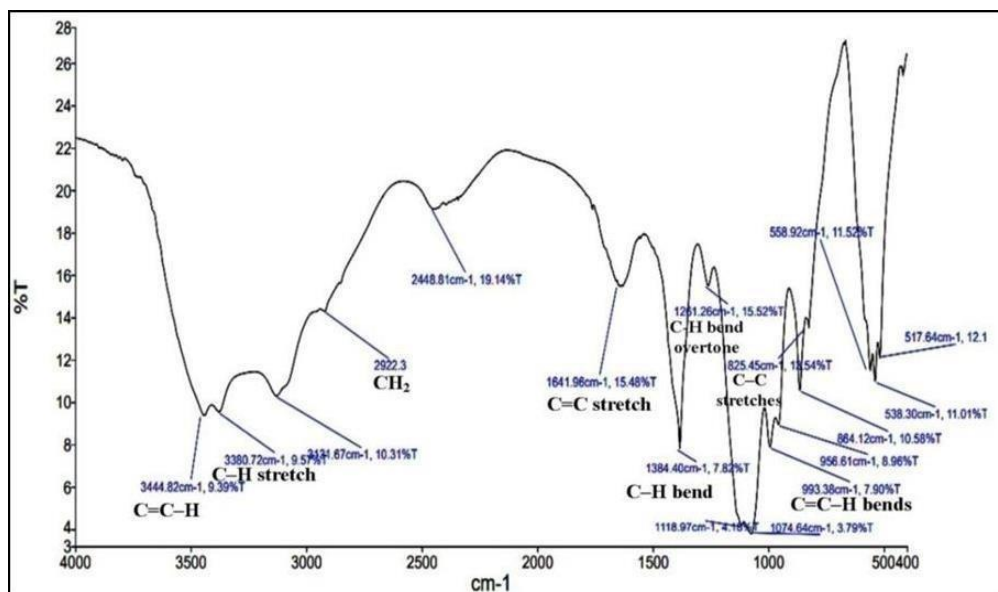


Fig. 4.11 FTIR spectra of Ag NPs indicating the functional groups present in the capping agent

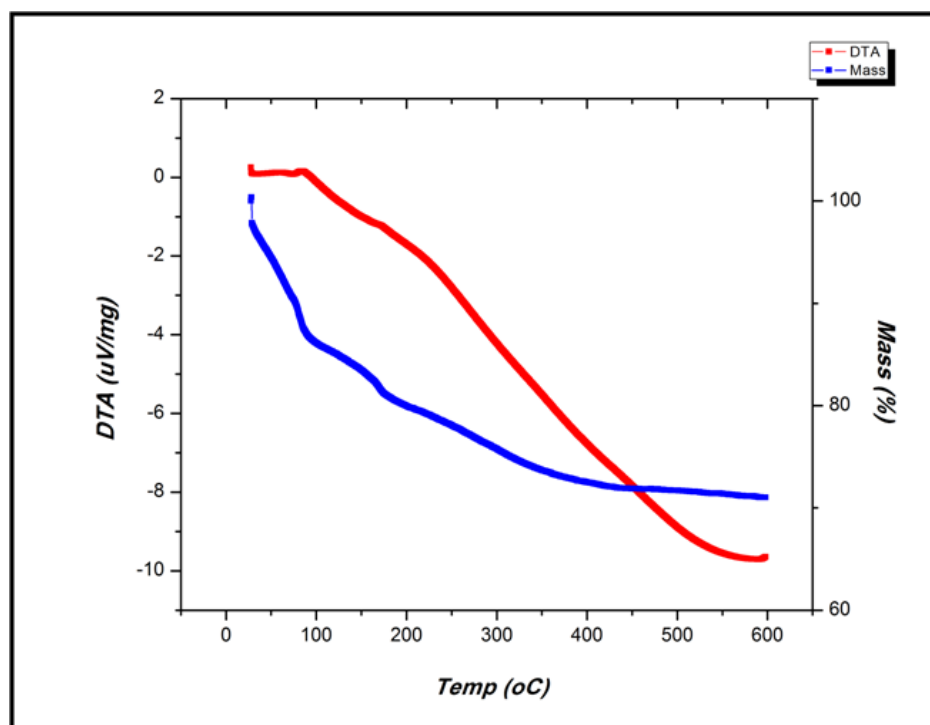


Fig. 4.12 DTA-TGA graph of Ag NPs showing the gravimetric loss with respect to the change in temperature

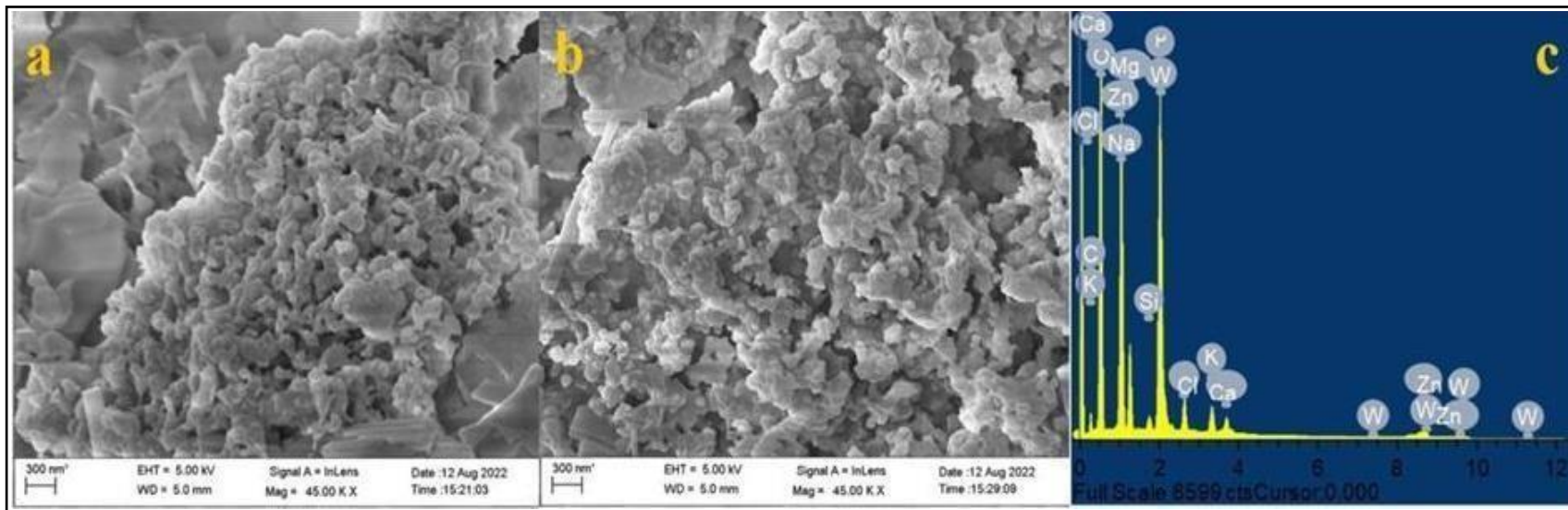


Fig. 4.13 SEM images of (a-b) ZnO NPs and (c) EDX spectra

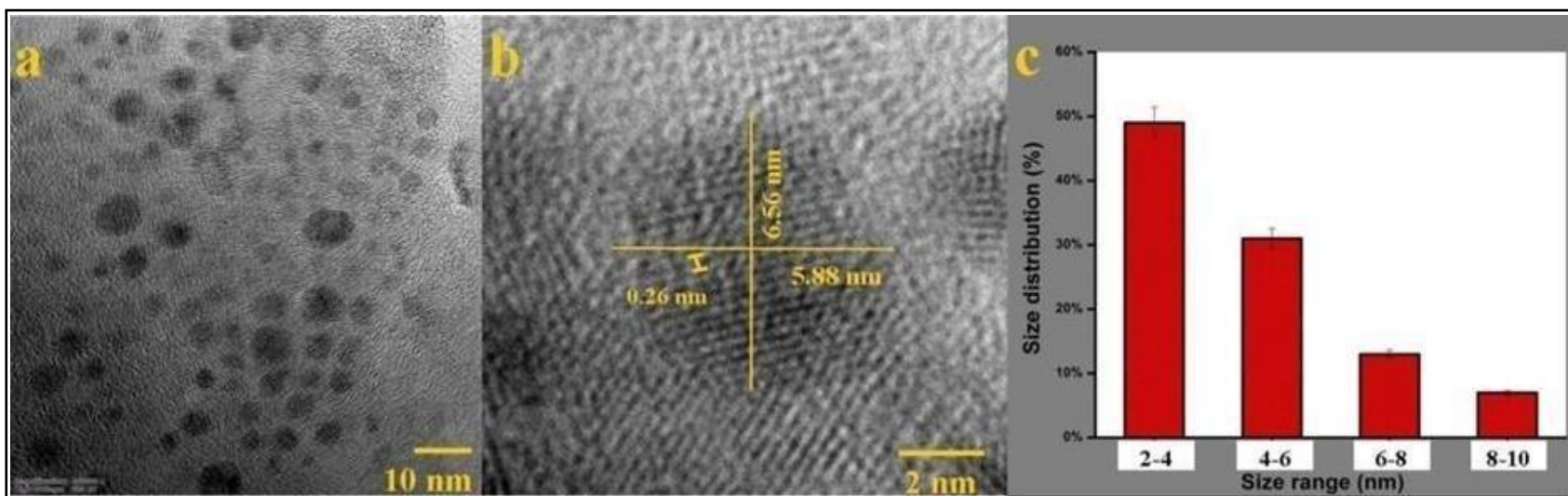


Fig. 4.14 TEM images of ZnO NPs at (a) low and (b) high magnification and (c) size distribution graph of the NPs

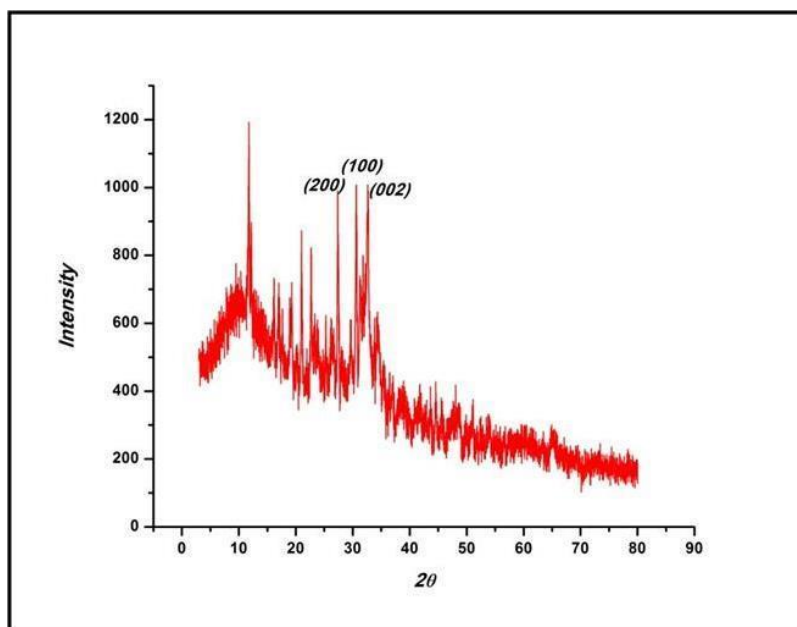


Fig. 4.15 The peaks obtained from XRD spectra showing the fcc lattice points in the ZnO NPs

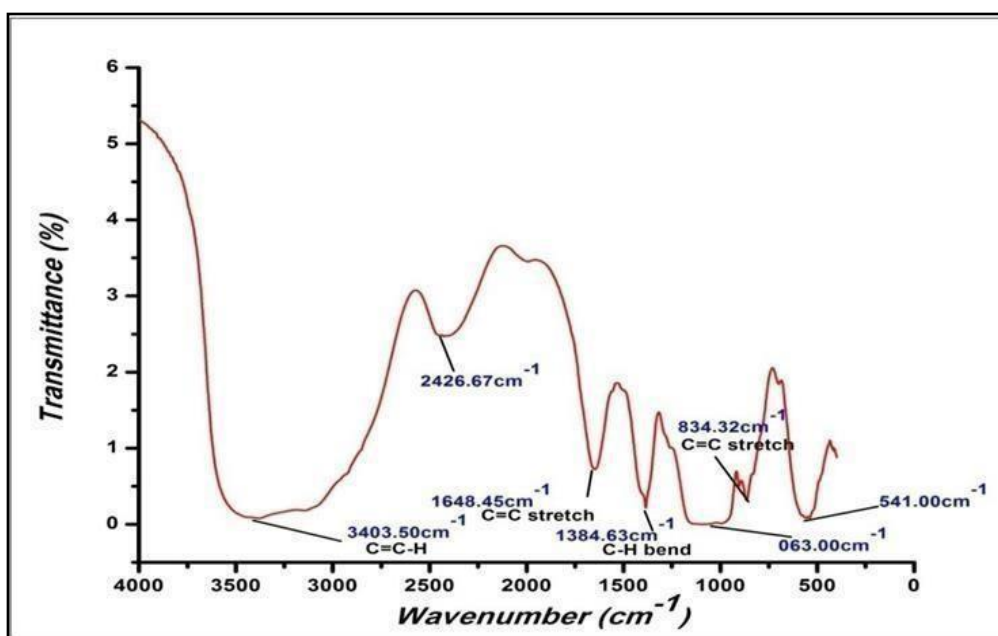


Fig. 4.16 FTIR spectra of ZnO NPs indicating the functional groups present in the capping agent

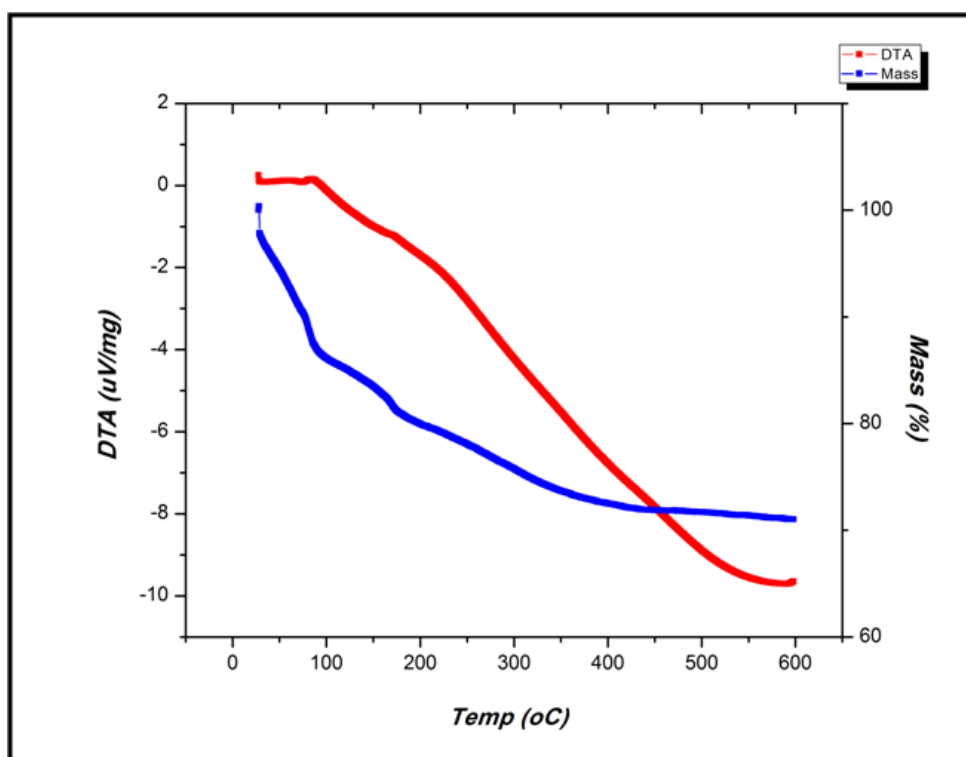


Fig. 4.17 DTA-TGA graph of ZnO NPs showing the gravimetric loss with respect to the change in temperature

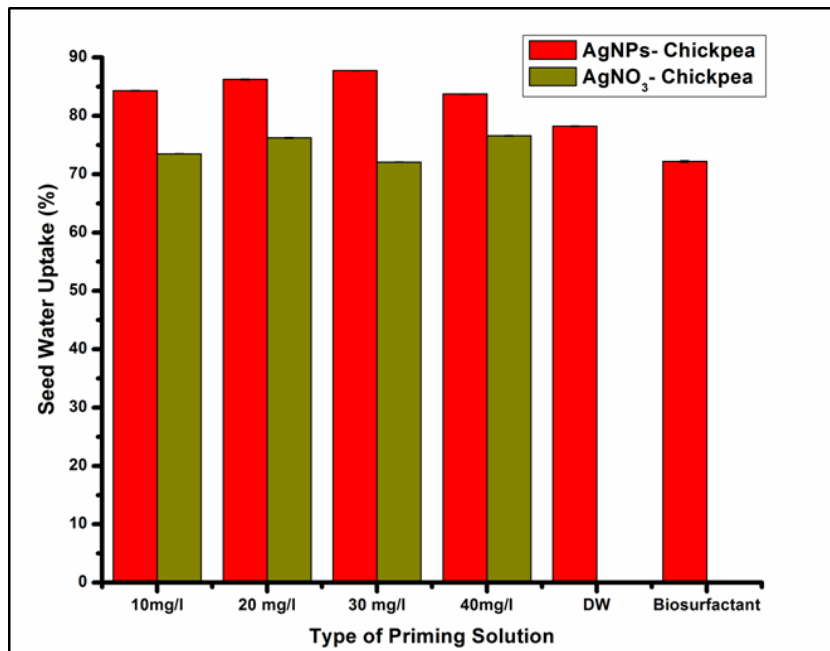


Fig. 4.18 Seed water uptake results of chickpea (*Cicer arietinum*) seeds after priming with various concentrations of Ag NPs. Where distilled water (DW) and biosurfactants are the control to see their effect on chickpea seeds

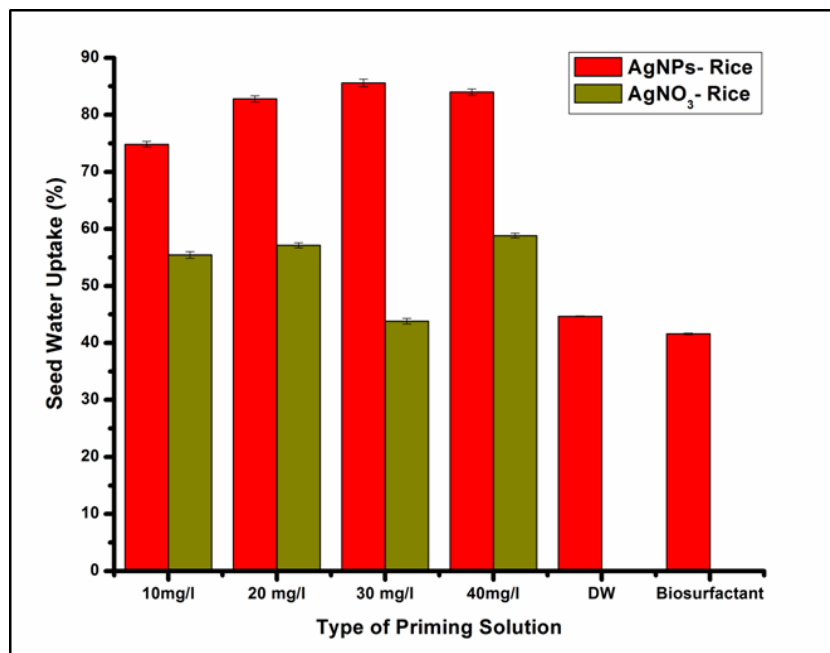


Fig. 4.19 Seed water uptake results of rice (*Oryza sativa*) seeds after priming with various concentrations of Ag NPs. Where distilled water (DW) and biosurfactants are the control to see their effect on rice seeds

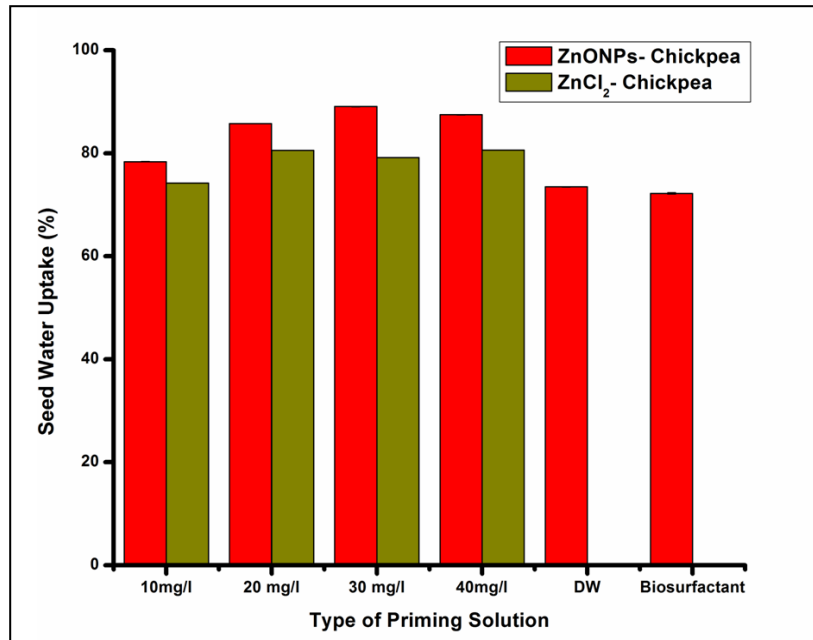


Fig. 4.20 Seed water uptake results of chickpea (*Cicer arietinum*) seeds after priming with various concentrations of ZnO NPs. Where distilled water (DW) and biosurfactants are the control to see their effect on chickpea seeds

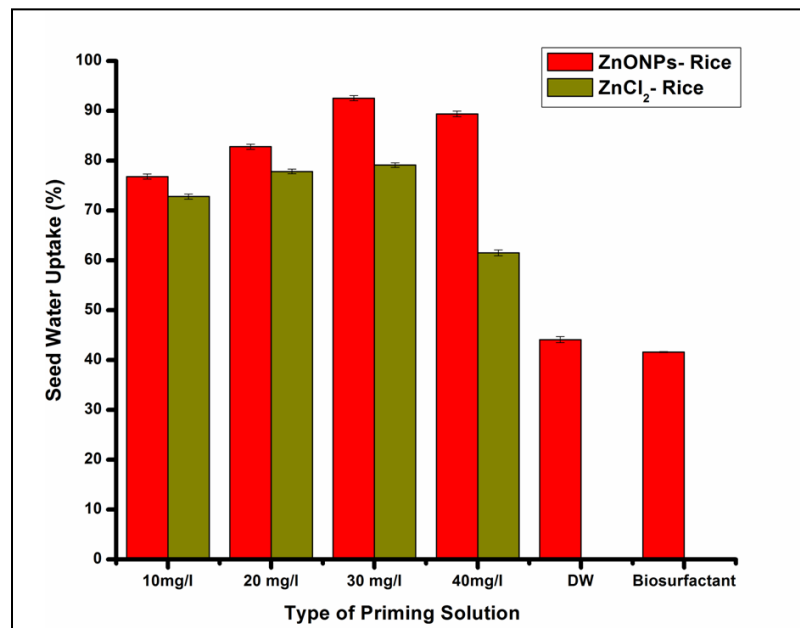


Fig. 4.21 Seed water uptake results of rice (*Oryza sativa*) seeds after priming with various concentrations of ZnO NPs. Where distilled water (DW) and biosurfactants are the control to see their effect on rice seeds

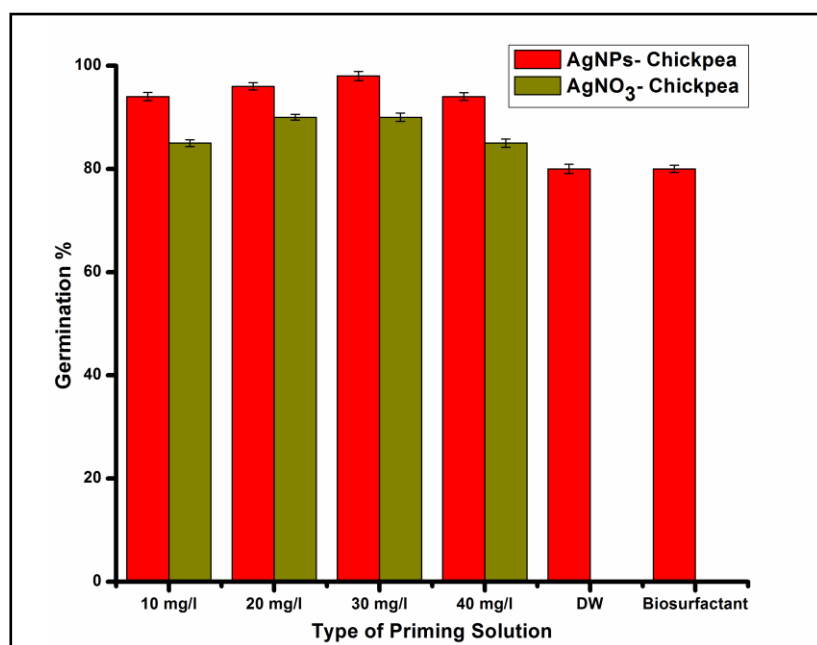


Fig. 4.22 Germination percentage of chickpea (*Cicer arietinum*) after priming with various concentrations of Ag NPs. Where distilled water (DW) and biosurfactants are the control to see their effect on chickpea seeds

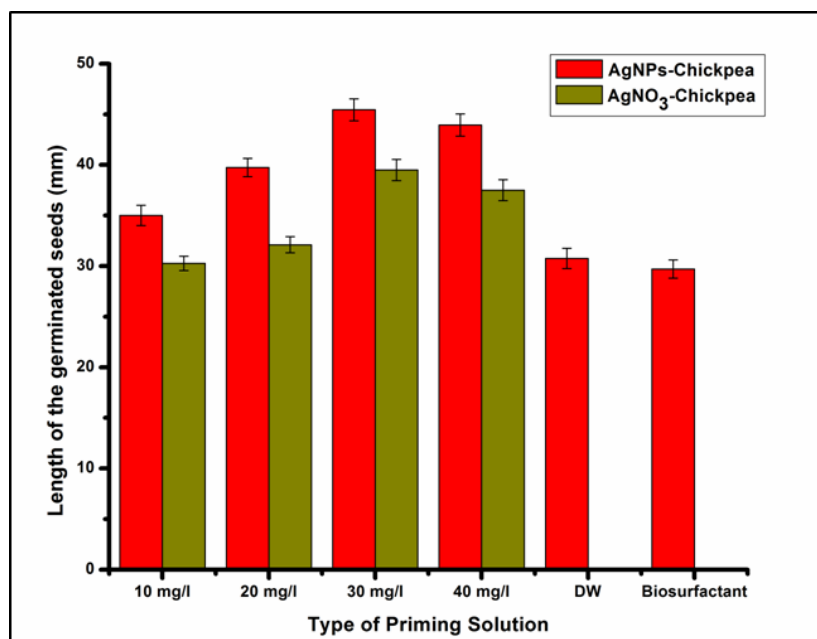


Fig. 4.23 Length of the germinated seedlings of chickpea (*Cicer arietinum*) seeds after priming with various concentrations of Ag NPs. Where distilled water (DW) and biosurfactants are the control to see their effect on chickpea seeds

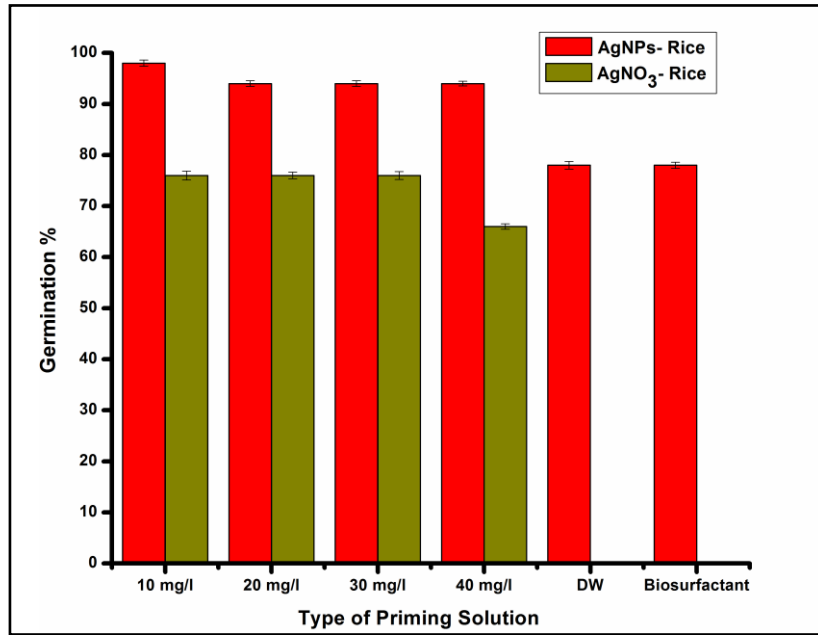


Fig. 4.24 Germination percentage of rice (*Oryza sativa*) seeds after priming with various concentrations of Ag NPs. Where distilled water (DW) and biosurfactants are the control to see their effect on rice seeds

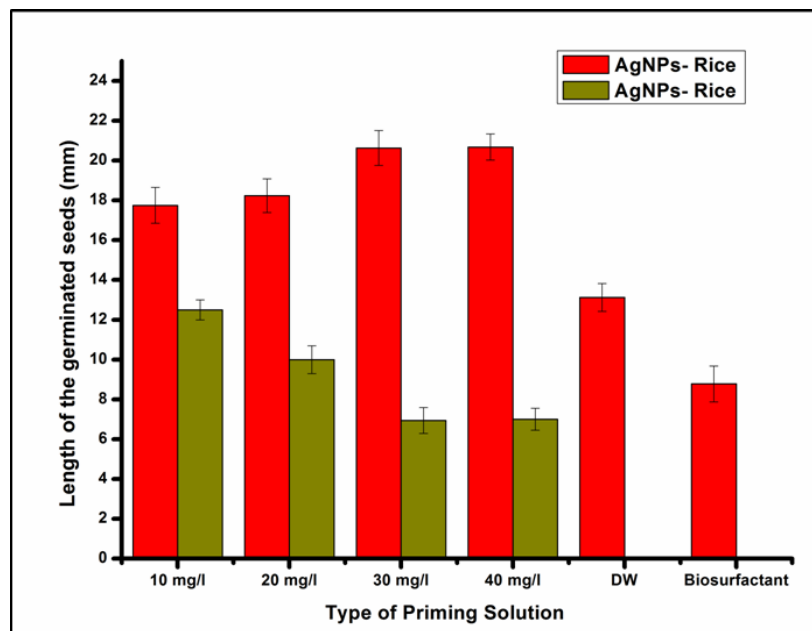


Fig. 4.25 Length of the germinated seedlings of rice (*Oryza sativa*) seeds after priming with various concentrations of Ag NPs. Where distilled water (DW) and biosurfactants are the control to see their effect on rice seeds

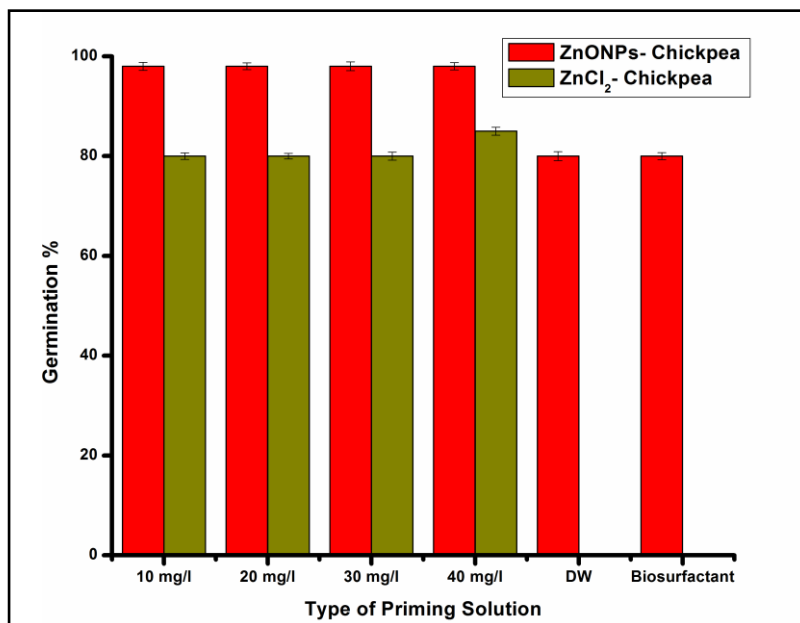


Fig. 4.26 Germination percentage of chickpea (*Cicer arietinum*) after priming with various concentrations of ZnO NPs. Where distilled water (DW) and biosurfactants are the control to see their effect on chickpea seeds.

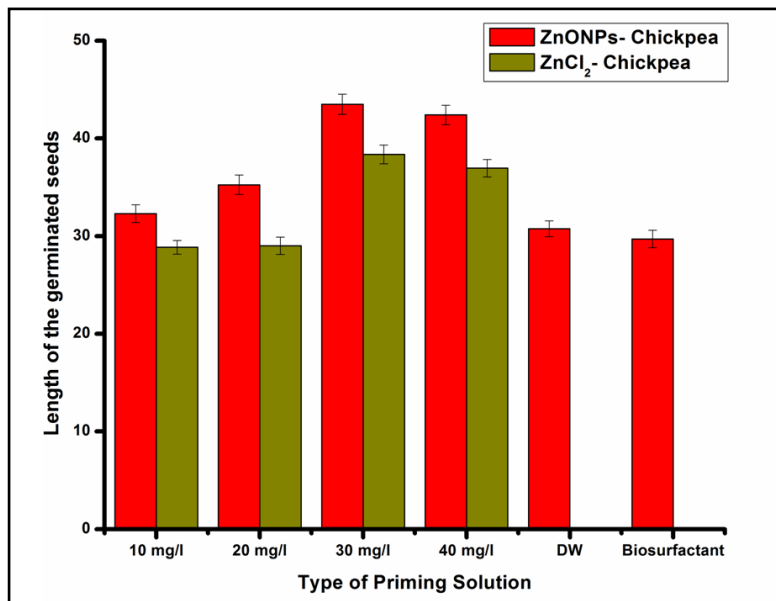


Fig. 4.27 Length of the germinated seedlings of chickpea (*Cicer arietinum*) seeds after priming with various concentrations of ZnO NPs. Where distilled water (DW) and biosurfactants are the control to see their effect on chickpea seeds

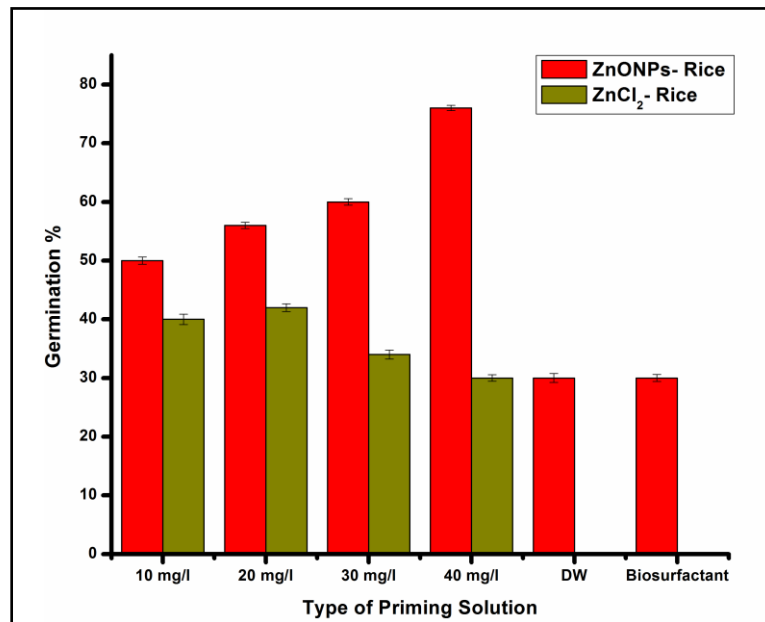


Fig. 4.28 Germination percentage of rice (*Oryza sativa*) seeds after priming with various concentrations of ZnO NPs. Where distilled water (DW) and biosurfactants are the control to see their effect on rice seeds

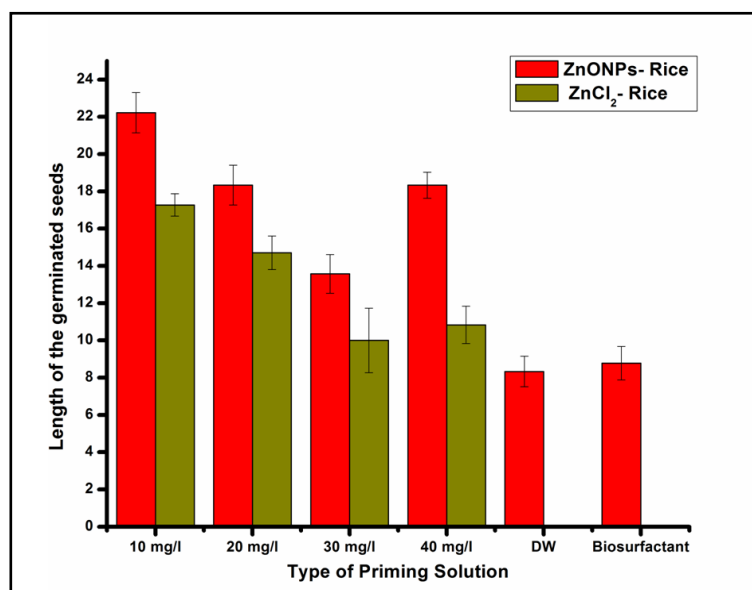


Fig. 4.29 Length of the germinated seedlings of rice (*Oryza sativa*) seeds after priming with various concentrations of ZnO NPs. Where distilled water (DW) and biosurfactants are the control to see their effect on rice seeds

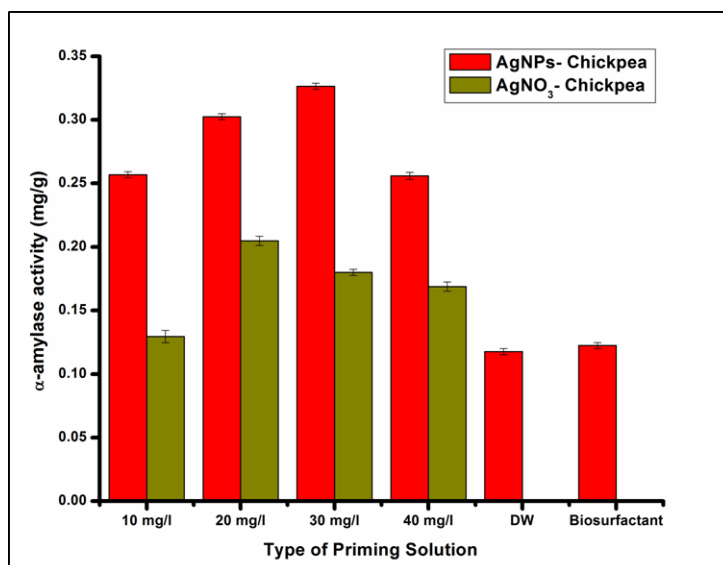


Fig. 4.30 Alpha amylase activity profile of chickpea (*Cicer arietinum*) seeds after priming with various concentrations of Ag NPs. Where distilled water (DW) and biosurfactants are the control to see their effect on chickpea seeds

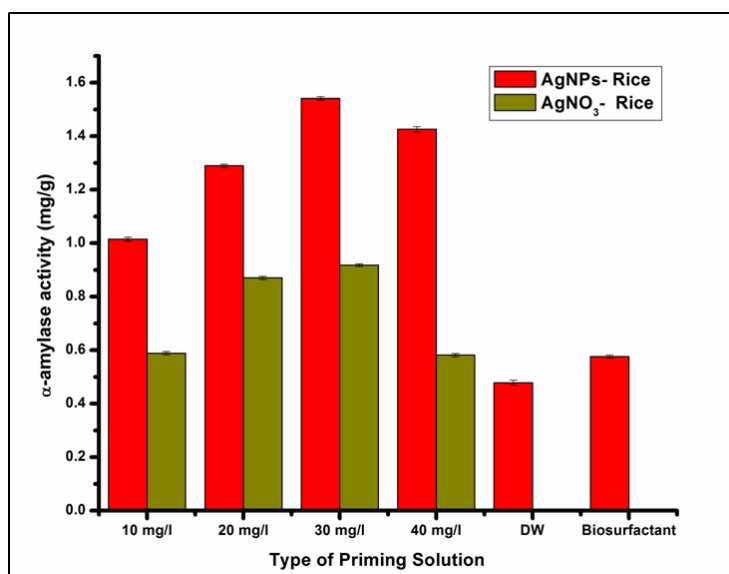


Fig. 4.31 Alpha amylase activity profile of rice (*Oryza sativa*) seeds after priming with various concentrations of Ag NPs. Where distilled water (DW) and biosurfactants are the control to see their effect on rice seeds

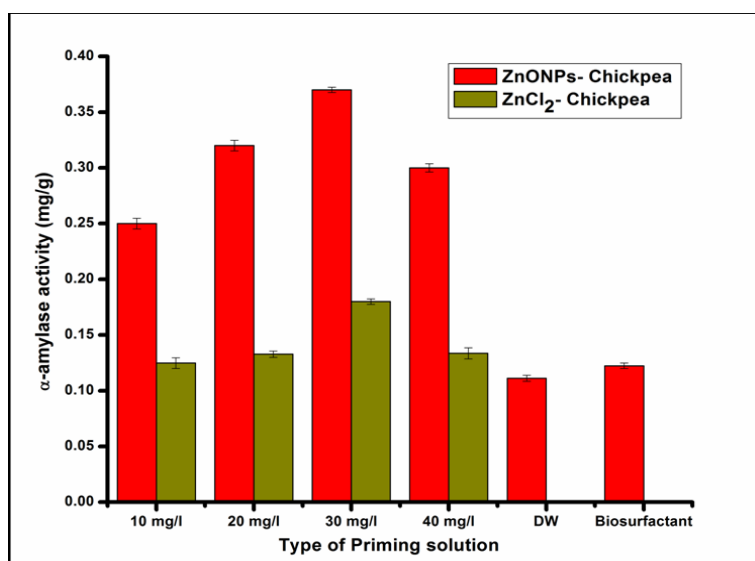


Fig. 4.32 Alpha amylase activity profile of chickpea (*Cicer arietinum*) seeds after priming with various concentrations of ZnO NPs. Where distilled water (DW) and biosurfactants are the control to see their effect on chickpea seeds

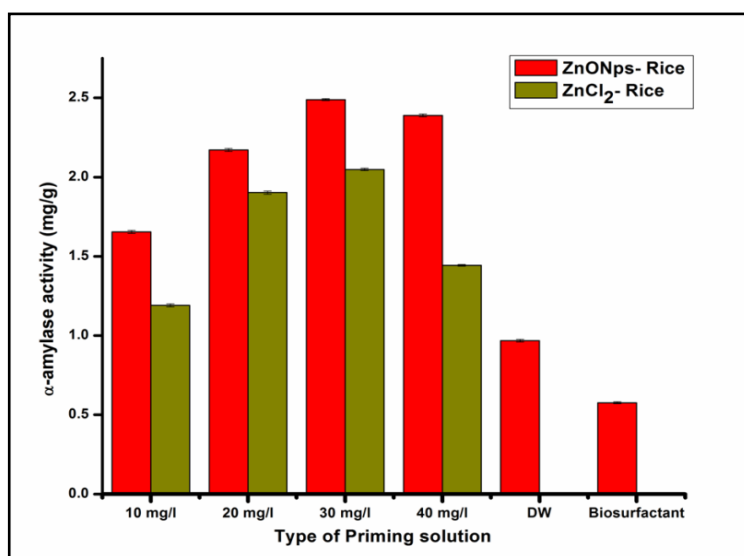


Fig. 4.33 Alpha amylase activity profile of rice (*Oryza sativa*) seeds after priming with various concentrations of ZnO NPs. Where distilled water (DW) and biosurfactants are the control to see their effect on rice seeds

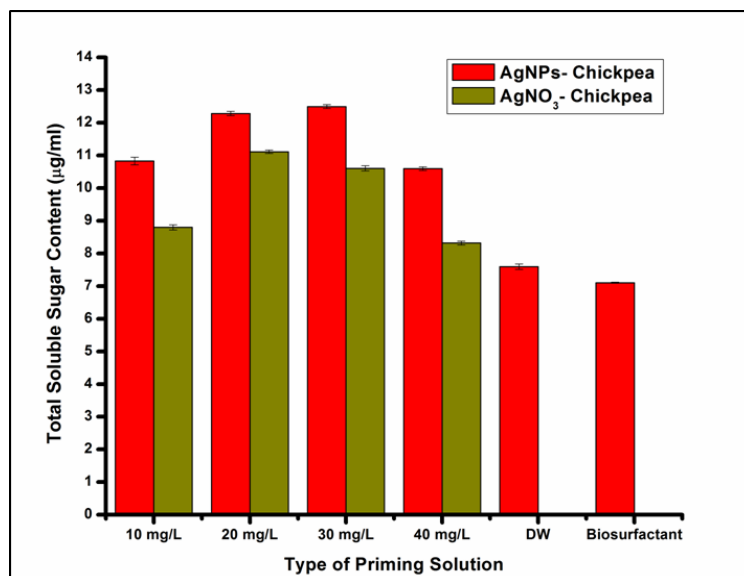


Fig. 4.34 Total soluble sugar of chickpea (*Cicer arietinum*) seeds after priming with various concentrations of Ag NPs. Where distilled water (DW) and biosurfactants are the control to see their effect on chickpea seeds

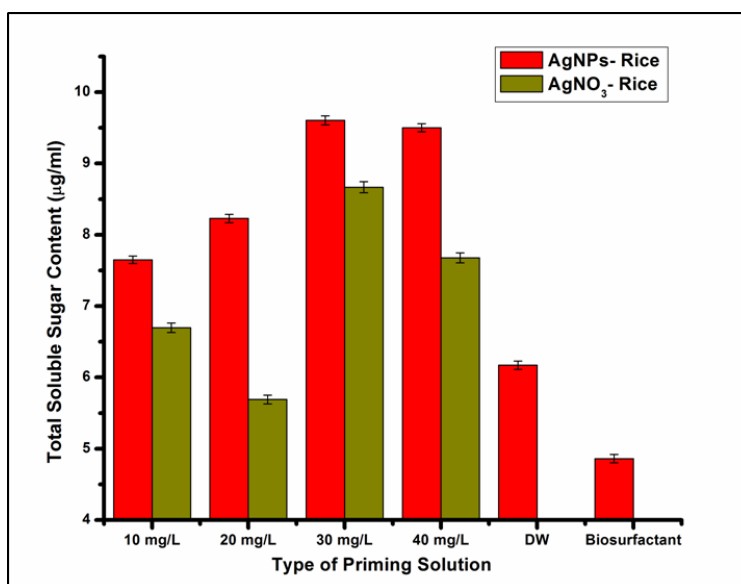


Fig. 4.35 Total soluble sugar of rice (*Oryza sativa*) seeds after priming with various concentrations of Ag NPs. Where distilled water (DW) and biosurfactants are the control to see their effect on rice seeds

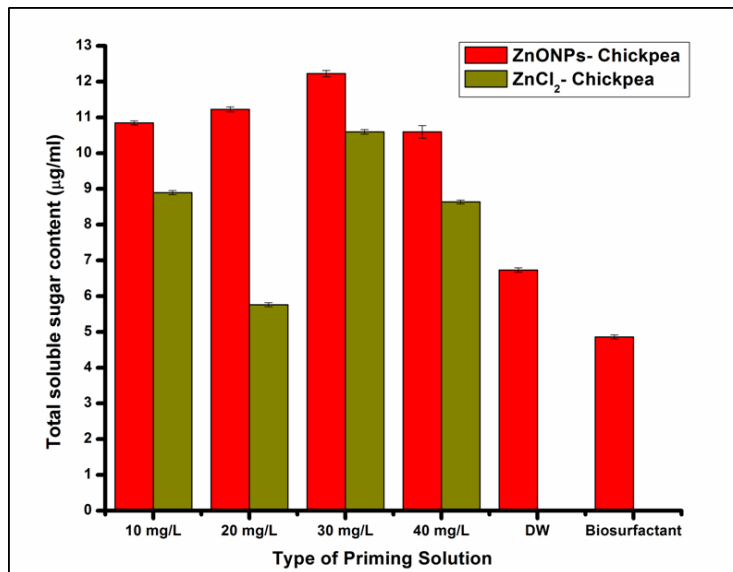


Fig. 4.36 Total soluble sugar of chickpea (*Cicer arietinum*) seeds after priming with various concentrations of ZnO NPs. Where distilled water (DW) and biosurfactants are the control to see their effect on chickpea seeds

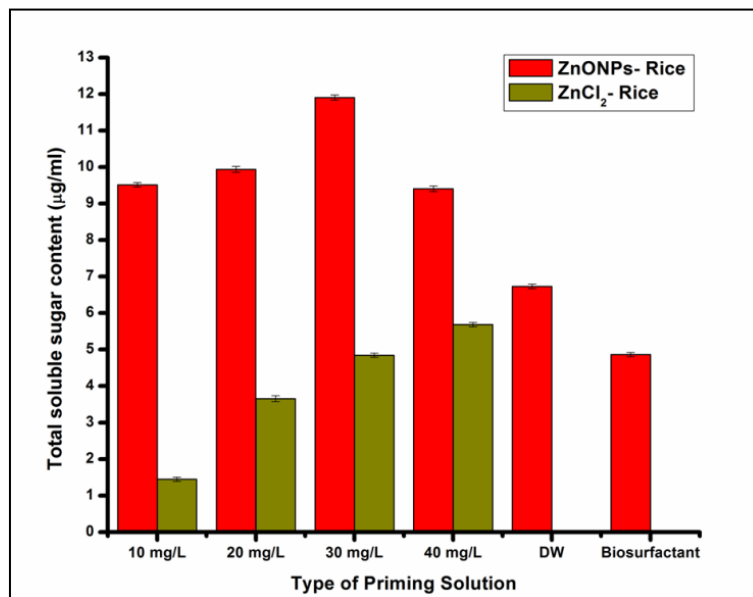
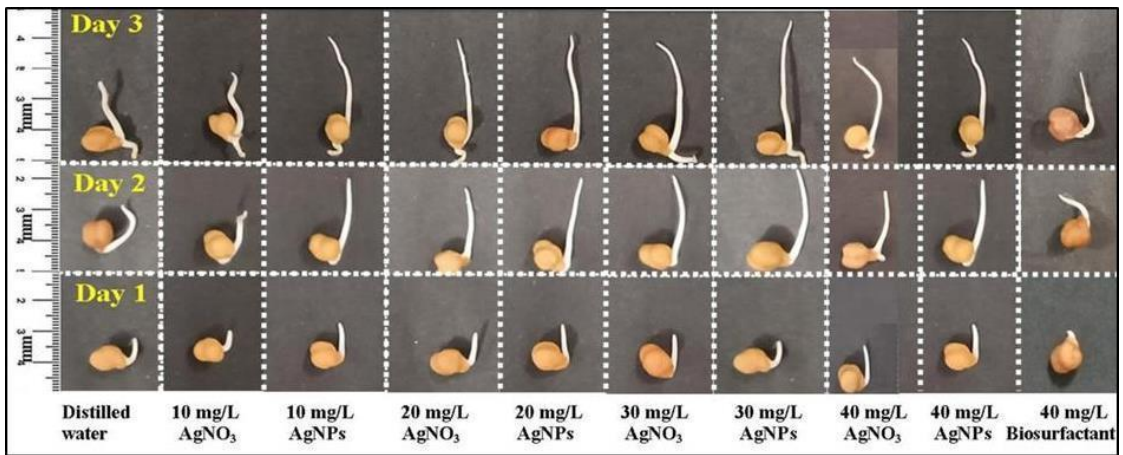
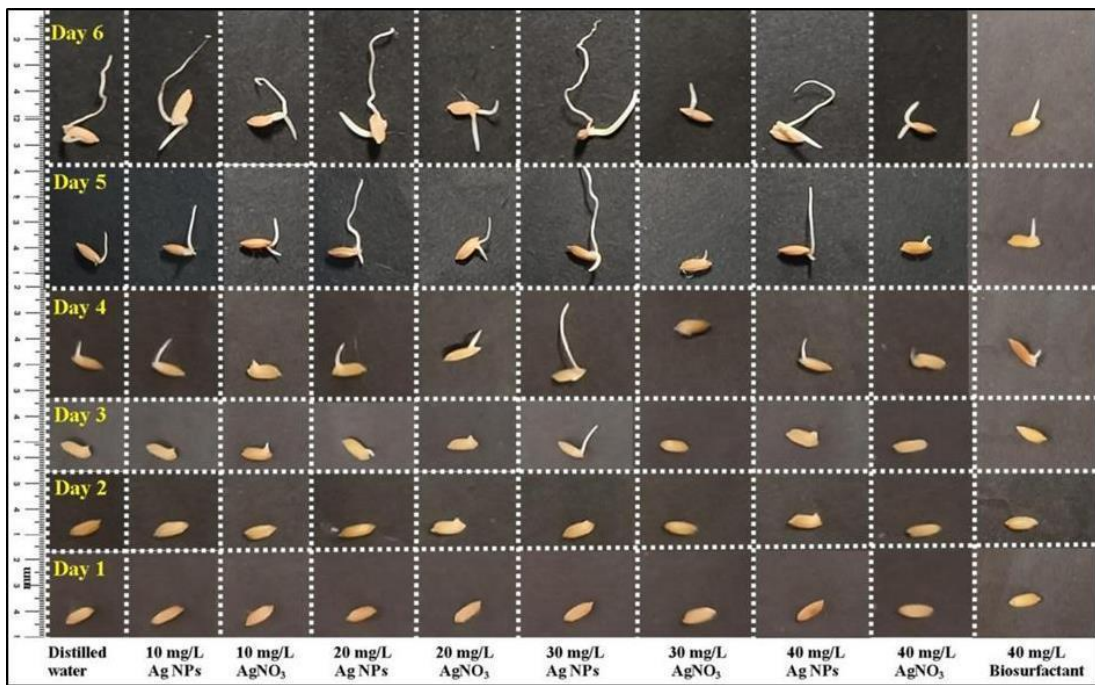


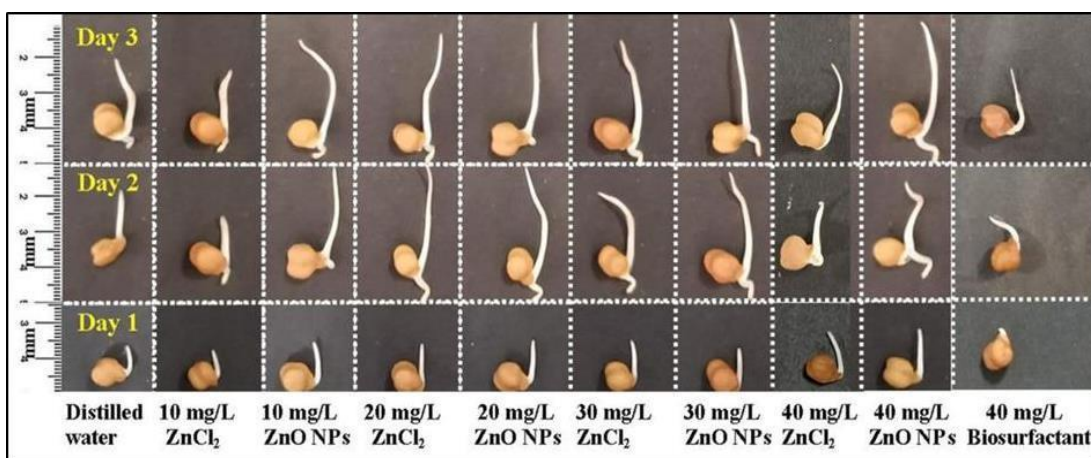
Fig. 4.37 Total soluble sugar of rice (*Oryza sativa*) seeds after priming with various concentrations of ZnO NPs. Where distilled water (DW) and biosurfactants are the control to see their effect on rice seeds



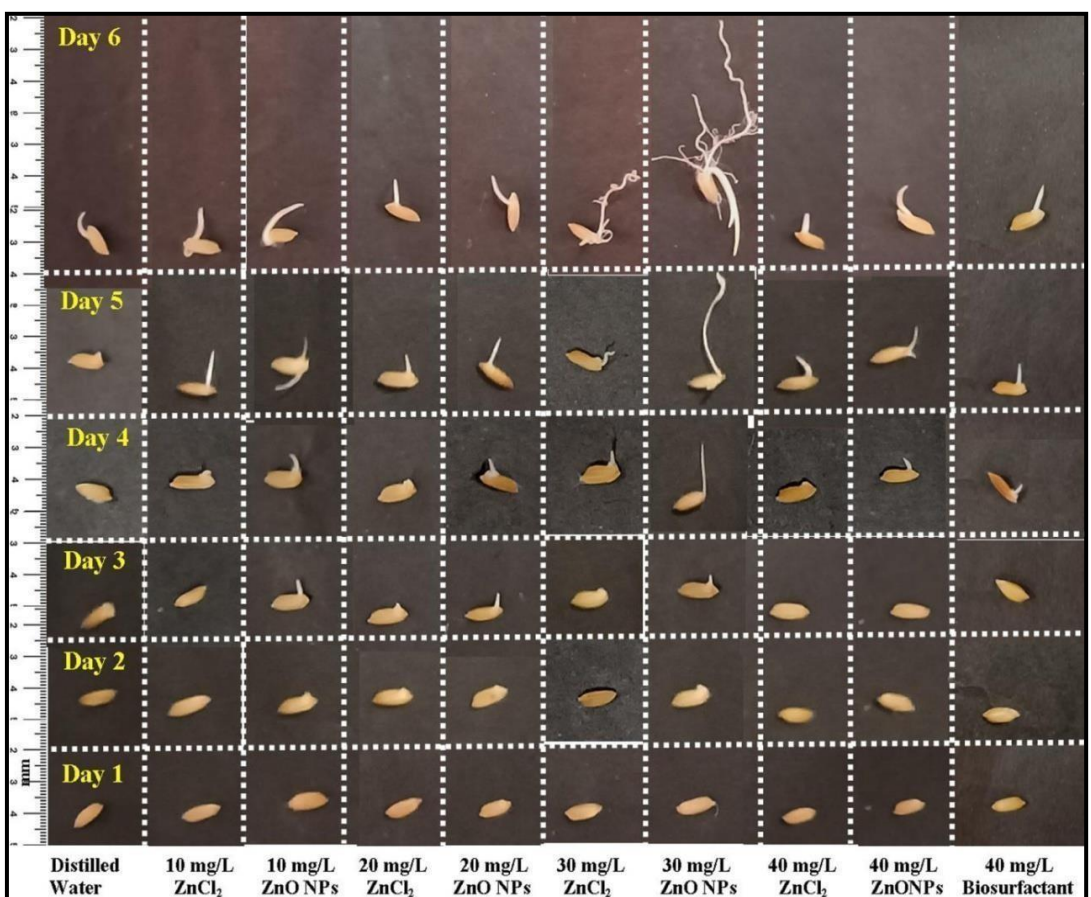
(a)



(b)



(c)



(d)

Fig. 4.38 Overall growth profile of (a) chickpea (*Cicer arietinum*) seeds after Ag NPs priming, (b) rice seeds (*Oryza sativa*) after Ag NPs priming; (c) chickpea seeds after ZnO NPs priming, and (d) rice seeds after ZnO NPs priming. Where distilled water and biosurfactant primed seeds are kept as control

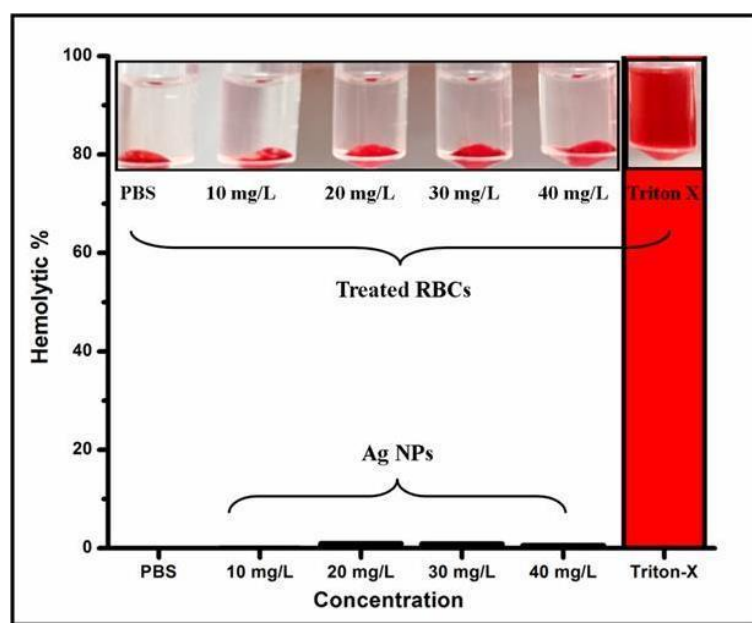


Fig. 4.39 Cytotoxicity assessment of various concentrations of Ag NPs on red blood cells. Where, PBS and Triton-X were used as negative and positive control respectively

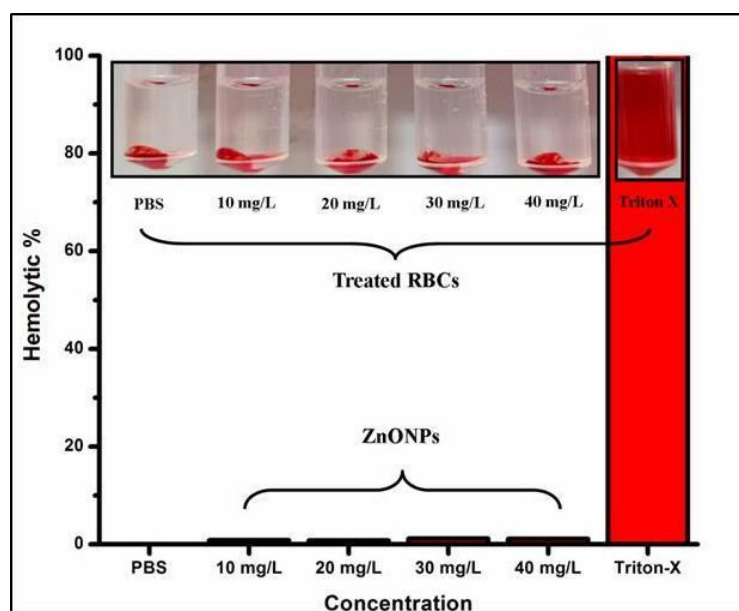


Fig. 4.40 Cytotoxicity assessment of various concentrations of ZnO NPs on red blood cells. Where, PBS and Triton-X were used as negative and positive control respectively

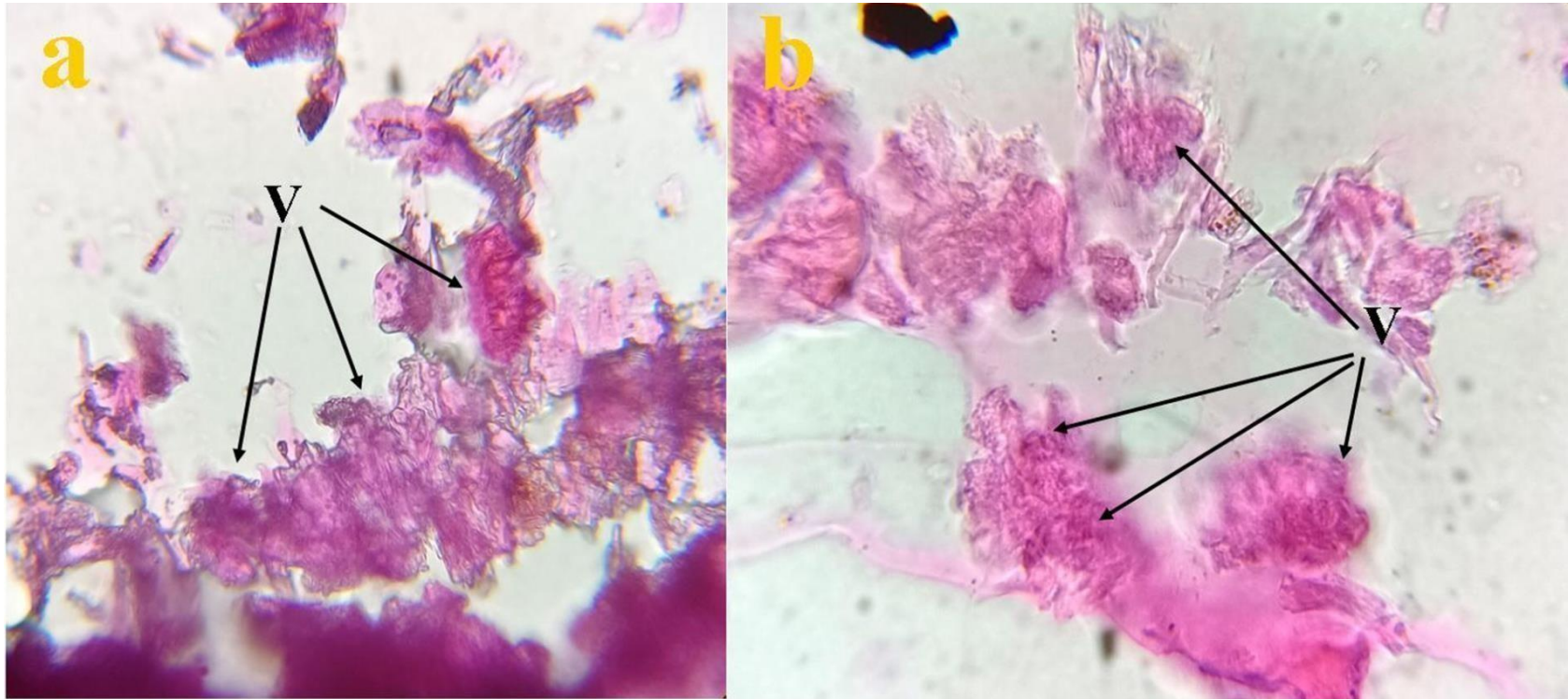


Fig. 4.41 Histological staining of the (a) control and (b) test (40 mg/L of Ag NPs) shows healthy gut of earthworm (*Eudrilus eugeniae*) with healthy villi (V)

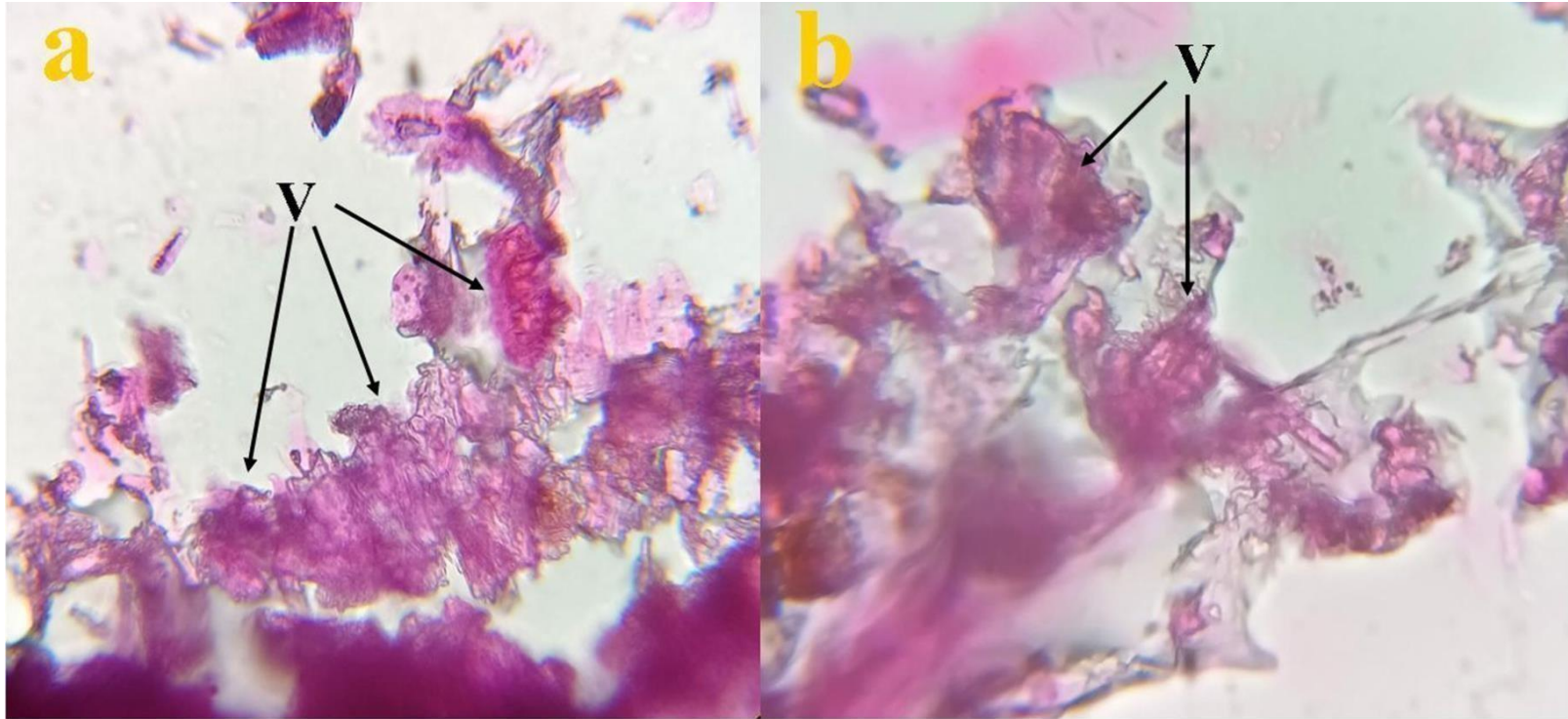


Fig. 4.42 Histological staining of the (a) control and (b) test (40 mg/L of ZnO NPs) shows healthy gut of earthworm (*Eudrilus eugeniae*) with healthy villi (V)

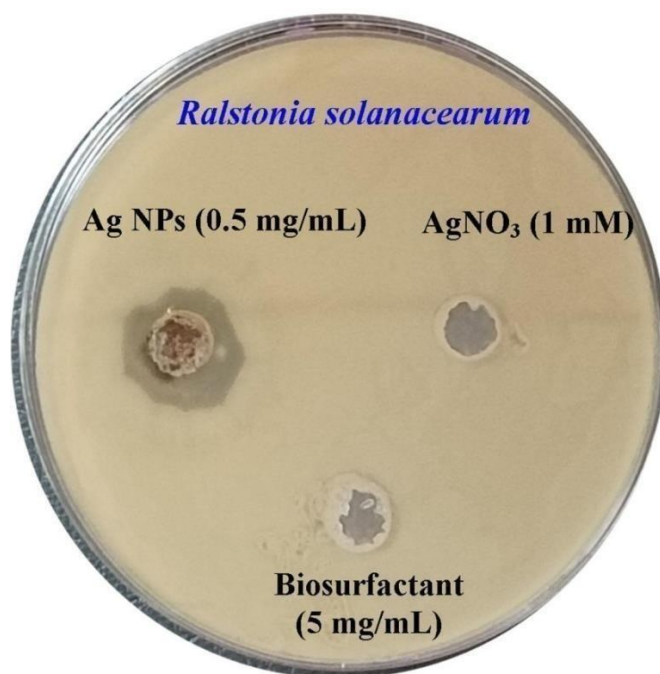


Fig. 4.43 A clear zone of inhibition exhibited by Ag NPs against *Ralstonia solanacearum* F1C1. Where, AgNO₃ and biosurfactant were used as control.

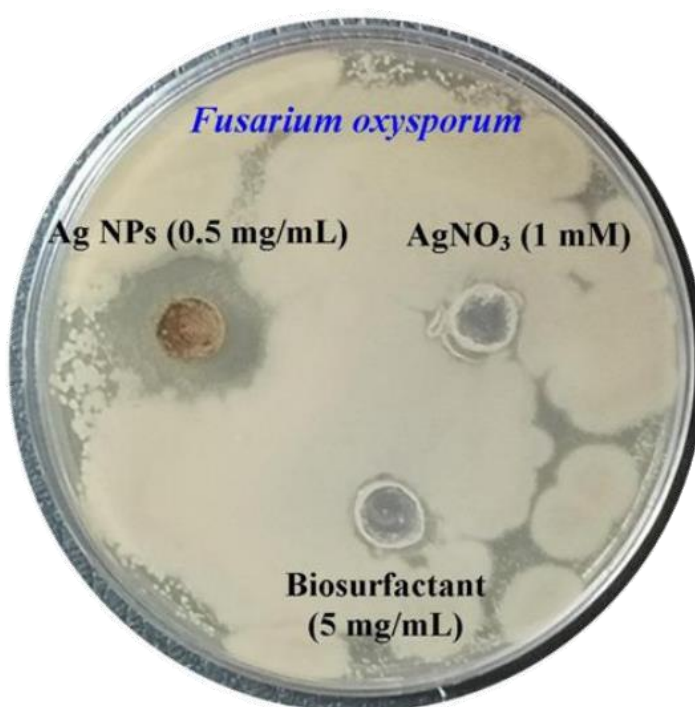


Fig. 4.44 A clear zone of inhibition exhibited by Ag NPs against *Fusarium oxysporum* f. sp. *pisi* (van Hall) Synder & Hansen strain 4814. Where, AgNO₃ and biosurfactant were used as control.